Trottier Annie-Pier (Orcid ID: 0000-0002-7596-8812)

MORPHOLOGICAL SIGNATURES OF DEGLACIATION AND POSTGLACIAL SEDIMENTARY PROCESSES IN A DEEP FJORD-LAKE (GRAND LAKE, SOUTH-EASTERN LABRADOR)

Annie-Pier Trottier[1,2*], Patrick Lajeunesse[1,2], Antoine Gagnon-Poiré[2,3] & Pierre Francus[2,3]

[1] Département de géographie, Université Laval, Québec, QC, Canada
[2] Centre d'études nordiques (CEN), Université Laval, Québec, QC, Canada
[3] Institut national de recherche scientifique (INRS), Centre Eau Terre et Environnement, Québec, QC, Canada

*Author contact:

email :annie-pier.trottier.1@ulaval.ca / Tel. 514-979-0474

Conflict of interest statement: There are no conflict of interest to declare.

Data availability statement: Research Data are not shared.

ABSTRACT

High-resolution multibeam bathymetric data and acoustic sub-bottom profiles were recently collected in Grand Lake (Labrador), one of the deepest lake basins in eastern North America, to reconstruct: (1) the retreat of the Laurentide Ice Sheet (LIS) west of Lake Melville, and (2) the history of sedimentation since deglaciation in this 54-km long, 3-km wide fjord-lake. Our results provide a morphostratigraphical framework that brings new insights to the style and pattern of retreat of the LIS in the region as well as deglacial and postglacial sedimentary dynamics. Terrestrial glacial lineations observed on a digital elevation model (DEM) provide evidence of a previously undocumented ice stream in the Grand Lake area. This newly mapped

ice stream suggests that the calving bay formed in Lake Melville triggered a reorganisation of the regional drainage pattern of the LIS. The sedimentary infill of Grand Lake consists of a sequence of deglacial to postglacial sediments that contain deposits related to a series of mass movements. The 8.2 cal ka BP cold event is recorded in Grand Lake by a series of closely spaced moraines deposited at the outlet of the fjord-lake to form a morainic complex similar to the Cockburn morainic complex on Baffin Island. During deglaciation, a dense dendritic network of proglacial gullies incised into the steep sidewalls of the lake. Since deglaciation, paraglacial and postglacial sedimentation has led to the deposition of large prograding deltas at the fjord head, where density currents remain active today and have formed a series of sediment waves on the frontal slopes and a prodeltaic environment.

Key words:

Geomorphology, deglacial landforms, fjord-lake, ice-stream, bathymetry

INTRODUCTION

Fjords and fjord-lakes are structurally controlled overdeepened valleys that have been carved over successive glaciations and ultimately drowned to form deep depositional basins at the interface between oceans and continents (e.g., Syvitski et al., 1986; Syvitski & Shaw, 1995; Aarseth, 1997; Evans, 2003; Glasser & Ghiglione, 2009; Hjelstuen et al., 2009; Lajeunesse, 2014; Brouard & Lajeunesse, 2019). Their morphology creates efficient sediment traps that can contain long-term sedimentary records of Quaternary environmental change (e.g., Mullins & Hinchey, 1989; Eyles et al., 1990; Eyles et al., 1991; Ó Cofaigh, 1998; Van Rensbergen et al., 1998; Cowan et al., 2010; Forwick et al., 2010; Hjelstuen et al., 2013; Lajeunesse et al., 2017) and catastrophic events (e.g., Beck et al., 1996; Bertrand et al., 2008; Fanetti et al., 2008; Hilbe et al., 2011; Praet et al., 2016). The high depositional rate observed in many fjords also allows the high-resolution reconstruction of past sedimentation patterns (Syvitski & Shaw, 1995). These drowned glacial valleys can be disconnected from the sea to form fjord-lakes via a forced-regression induced by glacio-isostatic rebound (e.g., Syvitski et al., 1986; Evans, 2003).

Fjords and fjord-lakes can be subject to high sedimentation rates, especially during deglaciation, and they are characterised by steep sidewalls; as such, these sidewalls are prone to sediment failure (e.g., Syvitski et al., 1986; Syvitski & Shaw, 1995; Syvitski & Shafer, 1996; Hampton et al., 1996; Girardclos et al., 2007; Fanetti et al., 2008; Cowan et al., 2010; Brouard

& Lajeunesse, 2019). Mass-movement deposits may thus be important components of the deglacial, paraglacial and postglacial sedimentary sequence of fjords and fjord-lakes (Bertrand et al., 2008; Fanetti et al., 2008; Hilbe et al., 2011; Praet et al., 2016). However, the frequency of mass movements and the associated trigger mechanisms can vary through time and space depending on the setting of each fjord; these factors include relative sea level (RSL) change, the proximity to an active seismic zone, sedimentation rates, wave activity, salinity, and water temperature (e.g., Mullins & Halfman, 2001; Overeem & Syvitski, 2010; Howe et al., 2010; Stocker et al., 2010; Van Daele et al., 2013). It is therefore important to understand those gravity-driven processes acting in a fjord to establish its sedimentary regime in support of interpreting the regional palaeoenvironmental record.

Hydroacoustic surveys using high-resolution swath bathymetry provide a full lake-bottom coverage for a detailed analysis of morphology and the production of geomorphological maps (e.g., Hilbe & Anselmetti, 2014; Dowdeswell et al., 2016; Batchelor et al., 2018; Lajeunesse et al., 2017; Trottier et al., 2018). Acoustic sub-bottom profiles reveal the sedimentary sequence and help identify stratigraphic units through their acoustic properties, architecture and relative position (e.g., Baeten et al., 2010; Forwick & Vorren, 2011; Waldman et al., 2010). Together, bathymetric data and sub-bottom profiles provide insight into past depositional dynamics, environmental change and sedimentary processes within a fjord basin (e.g., Forwick et al., 2010; Dowdeswell & Vasquez, 2013; Kempf et al., 2013; Dowdeswell et al., 2016). Such an approach in fjord-lakes can reconstruct the geomorphological evolution of the basin since deglaciation and identify past and modern sedimentary dynamics (e.g., Gagnon-Poiré et al., 2018).

Fjords and fjord-lakes are ubiquitous in eastern Labrador (Syvitski et al., 1986), and their stratigraphic records contain the pattern of deglaciation; the evaluation of this record can identify potential climatic and topographic controls on the retreat pattern of the Laurentide Ice Sheet (LIS) margin (Gagnon-Poiré et al., 2018; Brouard & Lajeunesse, 2019). Since the pattern of glacier retreat can vary locally, analysing the morphosedimentary record of marine or lake basins is required to fully understand the complex pattern of deglaciation. Fjord-lakes were also subjected to highly variable water levels during the initial phases of glacio-isostatic rebound (e.g., Syvitski & Shaw, 1995), and their sedimentary record should therefore improve our understanding of the changes in the sedimentary regime related to the passage from a marine to a limnic environment in a context of a retreating ice margin (e.g., Gagnon-Poiré et

al., 2018). In addition, the analysis of the stratigraphic record can identify the dominant triggers of seabed instabilities for the deglacial, paraglacial and postglacial periods.

Grand Lake is located near Lake Melville, where Fulton & Hodgson (1979) proposed the existence of a calving bay during deglaciation. The retreat sequence of the LIS margin west of Lake Melville remains, however, poorly documented and questions remain: Was the ice retreat rapid or episodic? Were there catastrophic events during the ice retreat? Was the terrestrial retreat of the LIS margin concomitant to the retreat into the fjord? Grand Lake is ideally located to answer these questions since it contains a thick sedimentary succession that likely recorded past environmental changes and geological events in its watershed. The morphosedimentary record of Grand Lake, through the analysis of swath bathymetry and sub-bottom profiles, provides a refined LIS deglaciation model for eastern Labrador and can define the influence of the Melville calving bay on the pattern of regional deglaciation. In this paper, we present recently acquired high-resolution swath bathymetry imagery and acoustic sub-bottom profiles from Grand Lake (Labrador) to: (1) provide a geomorphological map and a stratigraphic framework for the lake basin; (2) reconstruct the Late Pleistocene and Holocene evolution of the basin in relation to glaciation, deglaciation and glacio-isostatic rebound; (3) identify the activity of mass movements within this deep lake since deglaciation; and (4) identify postglacial sedimentary processes.

REGIONAL SETTING

Lake physiography

Grand Lake is a former fjord located in south-eastern Labrador (Canada) that is deeply incised into the Grenville province of the Canadian Shield (Figure 1). The fjord-lake is 54-km long, ≤3-km wide and follows a NW–SE alignment (Figure 2). This fjord-lake has a surface area of 150 km^2 and is situated at 15 m above sea level (asl). The lake is part of the Lake Melville watershed and is connected to Lake Melville by the 4-km long tidal Little Lake. Many small streams also enter along the fjord axis, and another tributary valley joins the fjord 17-km upstream from its outlet into Lake Melville (Figure 2). The fjord-lake is bordered by a few cliffs and mountains ≤400-m high. Grand Lake is also crossed at three locations by faults (Figure 2) formed by an allochthon boundary thrust of the Grenville Orogen (Green, 1974; Wardle et al., 1997; Lucas & St-Onge, 1998). Fulton (1986) and Vilks et al. (1987) mapped glacial lineations in the valley. The marine limit reached 150 m asl in the area, i.e., 135 m above

the present-day lake level, and extended upstream into the modern valleys of the Beaver and Naskaupi rivers (Fizthugh, 1973), the two main tributaries located at the head of the fjord.

Deglaciation history

During the last glaciation, eastern Labrador was inundated by the Quebec-Labrador Sector of the LIS, which extended offshore into the Labrador Sea (Dyke, 2004; Peltier, 2004; Occhietti et al., 2011; Peltier et al., 2016) and reached the edge of the continental shelf (Josenhans et al., 1986). During its retreat, the LIS margin stabilised 4 km east of the Grand Lake-fjord terminus at ~8.45 cal ka BP, depositing the Sebaskachu moraine (Figure 1, 2; Blake, 1956; Fulton & Hodgson, 1979; Dyke, 2004). The Grand Lake glacial valley was invaded by a deglacial sea as the LIS margin retreated toward the north-west. Fizthugh (1973) studied many sites of early human occupation and dated the occupied and abandoned settlements to analyse palaeoenvironmental change and marine limit variations in the Grand Lake area. The former fjord disconnected from the sea ~3 ka BP due to glacio-isostatic rebound to form the Grand fjord-lake (Fizthugh, 1973). Since the establishment of postglacial freshwater conditions, Grand Lake has trapped sediments coming from various sources with only fine-grained suspended sediments exiting the basin (Syvitski & Lee, 1997).

Regional palaeoenvironmental studies

Previous palaeoenvironmental studies in the area focused mostly on the Labrador Shelf and Lake Melville (e.g., Josenhans et al., 1986; Syvitski & Lee, 1997; Andrews et al., 1999). Lake Melville forms a large (2,100 km^2), semi-enclosed estuarine basin, located downstream of Grand Lake, that was subjected to a complex pattern of retreat of the LIS margin, characterised by many surrounding ice flows having various orientations (Syvitski & Lee, 1997), and the calving bay formed as the ice margin retreated (Andrews et al., 1999). The reconstructed LIS deglacial sequence in Lake Melville is based on the analysis of seismo-stratigraphic profiles (Syvitski & Lee, 1997) from which five seismic units were interpreted (maximum thickness): ice-contact (65 m), ice-proximal (238 m), ice-distal (290 m), paraglacial (57 m) and postglacial (44 m) sediments. According to these seismic units, the retreat of the LIS margin in the Lake Melville basin occurred in three major stages: (1) a tidewater glacier stage marked by multiple stabilisations, retreats and readvances of short-duration; 2) an enhanced ablation of the LIS characterised by high sedimentation rates that triggered mass movements; and 3) full deglaciation with lower sedimentation rates and the establishment of modern marine conditions (Syvitski & Lee, 1997). However, the context of the retreat of the LIS margin in Lake Melville

is unique due to the large size of this waterbody, its open connection to the Labrador Sea and the surrounding terrestrial multidirectional ice flows. The pattern and timing of ice retreat farther inland and upstream of Lake Melville remains undocumented.

METHODS

Hydroacoustic surveys were undertaken in Grand Lake in July 2016 to acquire high-resolution swath bathymetric imagery and sub-bottom profiles. Bathymetric data were acquired using a Kongsberg EM 2040C multibeam echosounder (300 kHz) and SIS™ software, coupled with a Kongsberg Seapath 330+ inertial navigation unit and GNSS antennas mounted on the 8-m long R/V *Louis-Edmond-Hamelin* research vessel (Université Laval). Depths were corrected using a Odom Digibar Pro (± 0.3 m·s^{-1}) sound velocity profiler. These data were post-processed using the Caris Hips and Sips™ 9.0 software and visualised using the QPS Fledermaus™ software. Geomorphological maps depicting sublacustrine landforms were produced using ESRI ArcGIS™ 10.2 software and a digital elevation model (DEM: resolution 20 m) provided by Department of Natural Resources, Government of Newfoundland and Labrador (https://gis.geosurv.gov.nl.ca/) coupled with a DEM derived from the swath bathymetric data. Data used for the location map (Figure 1) were provided by: (1) the General Bathymetric Chart of the Oceans (GEBCO) for elevation and bathymetry; (2) CanVec+ for shoreline and administrative data; and (3) Dyke (2004) for the positions of the LIS and Glacial Lake Agassiz-Ojibway.

Acoustic stratigraphy data were acquired using a Knudsen 3212 (3.5 kHz) sub-bottom profiler. Survey lines were arranged perpendicular to each other to determine the distribution of the acoustic units (Figure 2b). A sound velocity of 1,500 m/s was used to compute depths and calculate the thickness of the units. The SegyJp2Viewer™ software (NRCan) was used to analyse the sub-bottom profiles.

RESULTS

Bathymetry

Grand Lake is characterised by an elongate geometry, steep (slope ≤39°) bedrock sidewalls and a flat, deep central basin (≤245 m; Figure 2a). Based on the swath bathymetric data, the lake is divided into three sectors from west to east: (1) the deltas associated with the river mouths at the fjord head (Figure 3a); (2) the deep, nearly flat central basin (Figure 3b,c); and (3) the shallow, complex outlet of the lake (Figure 3d). The head of the fjord basin (Figure 3a)

is formed by two connected bays: a W–E elongated bay at the Beaver River mouth and a small N–S bay at the Naskaupi River mouth. At the junction of the two bays, the fjord is 145-m deep and slowly deepens south-eastward to its maximum depth (245 m), 23-km downstream in the central basin. The central basin (Figure 3b,c) forms the largest physiographic sector of the lake, representing half of the lake (28-km long). It is characterised by a nearly flat bottom floor (slope <1°; Figure 3c). Finally, a shallow complex bottom floor (≤190-m deep) having depositional lobes and ridges perpendicular to the fjord axis ends with a 13-m deep, 521-m wide central channel characterising the fjord outlet (Figure 3d).

Acoustic stratigraphy

Five acoustic units or subunits (U) were identified in Grand Lake based on their acoustic properties, geometry and stratigraphic position (Table 1): the U1 acoustic basement composed of till or bedrock; the U2a proximal and U2b distal glaciomarine units; the U3a distal paraglacial and postglacial lacustrine sediments; and the U3b deltaic paraglacial and postglacial sediments. These interpretations reflect previous acoustic stratigraphy studies in Quebec and Labrador lakes as well as adjacent continental margins (e.g., Syvitski & Praeg, 1989; Syvitski & Lee, 1997, Normandeau et al., 2013, 2017; Lajeunesse et al., 2017; Gagnon-Poiré et al., 2018; Trottier et al., 2018).

Acoustic Unit 1: acoustic basement

Unit 1 (U1) is the lowermost unit on the acoustic sub-bottom profiles; it is characterised at its surface by a high-amplitude continuous reflection showing some internal hyperbolae (Figure 4). Due to the acoustic attenuation in the sediments, U1 is visible mostly where the uppermost acoustic units are thin: along the margins of the lake, on the sidewalls or sills and ridges. The reflection is lost in the deep basin when buried underneath thick, younger acoustic units. U1 forms much of the sill near the south-eastern margin of the central basin and the ridges near the lake outlet.

The acoustic basement is interpreted as bedrock or ice-contact sediments (till) due to its relative position at the base of the stratigraphic sequence and on steep sidewalls. The 3.5-kHz signal of the sub-bottom profiler does not penetrate coarse sediments, which explains the high-amplitude reflection at the surface of U1 and the acoustic attenuation. U1 observed on the steep sidewalls is interpreted as bedrock, whereas the transverse sill and ridges within U1 are interpreted as morainic deposits. Some internal reflections observed within U1 at the south-eastern part of the lake are suggested to be internal stratifications. These internal stratifications may represent

different types of bedrock lithology or different depositional patterns of glacial diamicton; thus, the depositional origin of U1 may not always be the same.

Acoustic Unit 2: glaciomarine sediments

Unit 2 (U2) is observed in the deep central basin and on the shallow lateral shelves of all three sectors. U2 consists of two subunits having different acoustic properties. U2a comprises high-amplitude acoustic reflections that have unclear parallel, discontinuous reflections. U2b shows parallel reflections of medium-to-low amplitude that conformably drape the underlying unit and are interbedded by transparent layers. U2 is thinner near the fjord outlet (U2b ≤10 m) and thicker at the fjord head (U2b ≥35 m) near the fluvial inputs (Figure 4). Except on the shallow lateral plateau and near the lake outlet, acoustic attenuation in the sediments prevents the signal from reaching the base of U2 to observe the underlying unit. Therefore, it is not possible to determine the total thickness of U2 at the fjord head or in the deep central basin. However, Unit 2 is the thickest sedimentary unit observed from the available sub-bottom profiles of the lake.

U2a is only observed at the outlet of the lake near the morainic sills, where it reaches a maximum thickness of 20 m, whereas U2b is observed across the entire lake stratigraphy. U2b conformably drapes the underlying units (U1 and U2a), and its parallel reflections onlap the bedrock of the sidewalls. The onlapping geometry indicates that Unit 2 does not conformably drape the steep slopes, but rather it fills the deep trough of the fjord. In the deep central basin, acoustically transparent to chaotic layers and lenses are observed at various levels inside U2b (Figures 4b, 6a,b, 7b).

Strong acoustic reflections and high-amplitude parallel reflections are usually associated with coarse sediments deposited in a high-energy setting, such as a proglacial environment (e.g., Syvitski & Praeg, 1989; Cowan et al., 2010; Forwick & Vorren, 2010). The location of U2a near morainic sills and its internal high-amplitude acoustic reflections suggest that it was deposited in a proglacial sedimentary regime in a deglacial sea having a proximal ice margin. In such deglacial seas, the energy of the depositional environments decreases as the ice margin retreats (e.g., Syvitski, 1989). The deep and calm sedimentary environments in these seas are characterised by the slow settling of fine-grained sediments that fill the lower topography (Elverhøi et al., 1983; Mullins & Hinchey, 1989; Syvitski & Lee, 1997; Mullins & Halfman, 2001; Boyd et al., 2008; Hjelstuen et al., 2009; Stocker et al., 2009; Cowan et al., 2010; Waldman et al., 2010; Forwick & Vorren, 2010; Heirman et al., 2012; Turner et al., 2012; Hansen et al., 2013; Kempf et al., 2013; Van Daele et al., 2016). The rhythmicity and medium

amplitude of the reflections in U2b indicate a low-impedance contrast of the sediments interbedded with thin layers of higher contrast. Such a low-impedance contrast suggests an acoustic uniformity formed by sediments having a similar density or properties. Well-sorted sediments are deposited in low-energy environments in a context of deglaciation; such environments are associated with distal glaciomarine sedimentation, where the ice margin retreats inland, and sediment is transported into the basin from meltwaters (Syvitski et al., 1986; Syvitski & Shaw, 1995).

Acoustic Unit 3: paraglacial and postglacial sediments

Unit 3 (U3) is the uppermost unit and covers the entire lake floor at a maximum thickness of 10 m. U3 is divided into two subunits. U3a is formed of acoustically chaotic, stacked layers that have a high-amplitude hummocky reflection at the surface. U3b consists of closely spaced, high-amplitude parallel reflections that conformably drape the underlying unit. In U3a, the acoustically chaotic layers and their high-amplitude reflections are discontinuous and, in some cases, abruptly disrupted, i.e., the acoustic return is not always strong. U3b shows high-amplitude reflections at the fjord-lake head and in the deep central basin (Figure 4a,b) but presents low-amplitude reflections near the fjord-lake outlet (Figure 4c). The visual difference between the units is interpreted as the downsizing of grains away from the river mouths, with deposition of coarser sediments near the head of the fjord-lake and finer sediments toward the outlet. In the deep central basin, two large high-amplitude undulating reflections (5-m high, 500-m long) are observed inside U3, 18 km downstream the Naskaupi River mouth (Figure 4b). U3b is only observed at the river mouths on the deltas, and this subunit has a strong acoustic reflection at the surface and a sharp contact with the underlying unit, showing an erosional base at some sites. On the delta, the acoustic penetration into U3b increases moving away from the river mouth, suggesting a decrease in grain size.

U3 is interpreted as a paraglacial and postglacial sedimentary unit. The paraglacial period is associated with high sedimentation rates due to the fluvial remobilisation of glacial sediments deposited earlier within the watershed (Church & Ryder, 1972; Syvitski, 1991; Dietrich et al., 2017). The postglacial period is associated with low sedimentation rates of non-glacial processes, such as the modern fluvial seasonal discharge following the complete ablation of the LIS. The subunits U3a and U3b are associated with the same period of sedimentation, but they represent a lateral transition of the depositional system that follows the fjord axis with the proximal deltaic sediments at the head of the fjord (U3a) and the distal deposits downstream (U3b; Figure 5). The deltaic environments (U3a) are formed by: (1) coarse-grained sediments

on the delta tops and frontal slopes that prevent acoustic penetration; (2) buried organic content on the delta slopes that cause gas to accumulate and attenuate the acoustic penetration (Figure 4a); and (3) a stratified package of stacked mass-movement deposits (MMDs) that form acoustically chaotic layers at the toe of the delta.

Downstream in the basin, the acoustic facies (U3b) are more uniform having a depositional system associated with fine-grained sediments transported by interflows or underflows interbedded by the distal portion of turbidites to produce parallel acoustic reflections on the sub-bottom profiles (Figure 5). The variation in acoustic amplitude between U2b and U3b indicates a change in the depositional environment interpreted as a transition from a glaciomarine (U2) to a postglacial lacustrine (U3a) environment, where the isolated basin receives paraglacial sediments through fluvial transport. The high-amplitude undulating reflections observed within U3 are interpreted as buried sediment waves (Figure 4b). Paraglacial environments are usually characterised by high sedimentation rates due to the availability of glacial sediment in the landscape that can be easily eroded and transported by fluvial processes (Church & Ryder, 1972; Ballantyne, 2002). Past strong river inflows having a high sediment content as well as catastrophic events (flood or mass movement) can also produce strong density flows. Such density flows can be supercritical flows upon their entrance into the freshwater of a fjord-lake and can form large-scale sediment waves on the lake floor (Symons et al., 2016).

Deposits and landforms

Sediment waves

Deltas are located off both Beaver and Naskaupi river mouths and sediment waves are observed on their frontal slopes at a maximum depth of 133 m (Figure 6). The Beaver and Naskaupi delta slopes are ≤1.5° and ≤2.5°, respectively. The acoustic sub-bottom profiles show that sediment waves are present in U3a; these are thus interpreted to be composed of deltaic sediments. A higher concentration of sediment waves is observed on the upper slope in coarse sediments. Previous studies have demonstrated that seasonal fluvial pulse discharges can generate gravity flows (Desloges & Gilbert, 1998; Van Rensbergen et al., 1998; Gilbert & Butler, 2004; Gilbert et al., 2006) and form sediment waves on delta frontal slopes (Wynn et al., 2002; Girardclos et al., 2010; Hilbe & Anselmetti, 2014; Clarke et al., 2014; Normandeau et al., 2016; Symons et al, 2016). The activity of gravity flows as a trigger mechanism for such sediment waves fits with the morphostratigraphy of the deltas in Grand Lake as stacked mass-

transport deposits are observed in the deltaic unit (U3a). However, it is not possible to isolate the specific trigger mechanisms or the rate of migration as only one acoustic survey was made.

Sediment waves observed near Beaver River are not located at the river mouth but rather on the southern side of the bay (Figures 3a, 6a). These waves are draped by soft sediments (U3a) that smooth the landforms on the swath bathymetry imagery as opposed to the sharp, well-defined sediment waves on the Naskaupi River delta. Therefore, the sediment waves observed near the Beaver River probably indicate an ancient position of the river mouth since the river is known to meander. Sediment waves near the Naskaupi River mouth are interpreted as still active based on the absence of draping sediments on the acoustic sub-bottom profiles.

Gullies

The swath bathymetric imagery shows that a dense network of gullies incises 87% of the slopes in Grand Lake. The lateral sidewalls are completely incised by gullies, whereas only the river mouth and the lake outlet are not affected by gullying. The acoustic sub-bottom profiles show that gullies were carved in U1 and draped by U2 sediments (Figure 7). The thin cover of U2 on the sidewalls and its draping geometry impede the burial of the underlying landforms. Thus, the gullies incised in the basal U1 were preserved despite the subsequent sedimentation, and the landforms remain visible on the swath bathymetry imagery (Figure 7c). In the deep central basin, however, the glaciomarine-ponded sedimentation (U2) buried the basal portion of the gullies (Figure 7a,b).

Mass-movement deposits

Numerous scarps, lobes of debris and hummocky topographies of variable size are observed on the swath bathymetry imagery: (1) small-scale lobes at the toe of slopes at the head and outlet of the lake (Figure 3a–d); (2) hummocky topography at the fjord-lake head near the river mouths (Figure 3a); and (3) a large headscarp associated with a large chaotic deposit at the south-eastern margin of the central basin (Figures 3c and 8).

Many semi-transparent and lens-shaped layers are observed at various levels in U2 and U3 on the sub-bottom profiles (Figures 4a,b and 9). Frontal lobes, hummocky topography, headscarps and acoustically semi-transparent layers are typical characteristics of MMDs (e.g., Hampton & al., 1996; Hilbe et al., 2011; Moernaut & De Batist, 2011; Kempf et al., 2013). The observed mass-movement morphologies indicate that Grand Lake was exposed to gravity-driven processes. Three groups of MMDs are observed in Grand Lake (Figure 9): (1) small MMDs in U3 having an erosive base and a lens shape that pinches out away from the sidewall (Figure 9a); (2) stacked MMDs observed strictly in Sector A near the Beaver River mouth that are

characterised on sub-bottom profiles by a hummocky topography, chaotic internal acoustic reflections and an extension over the entire lake width (Figure 9b); and (3) a large-scale MMD (4.1 km^2) at the margin of the central basin; the chaotic bottom floor observed on the swath bathymetry imagery overlies an extensive acoustically semi-transparent layer on the sub-bottom profiles (Figures 8 and 9c).

The large and widespread MMD located along the south-eastern margin of the deep central basin is observed west of a large headscarp. The scarp is oblique to the lake axis on a low angle slope (<1°) and follows a fault formed during the Grenville Orogen. The hummocky deposits extend westward of the scarp (Figure 8). This widespread MMD is characterised by two different acoustic facies on the sub-bottom profiles: (1) a chaotic internal acoustic character having a hummocky topography near the scarp, and (2) a smooth westward transition to an acoustically transparent deposit marked by a flat topography. This MMD covers 4.1 km^2 on the swath bathymetric imagery and is buried under 14 m of draping, parallel reflections on the sub-bottom profiles. The sub-bottom profiles reveal that the MMD covers a wider extent than suggested by the swath bathymetry imagery as the topography of the overlying draped sediments flattens westward.

Moraines

A large ridge (1.6-km long, 100-m high) incised by gullies lies perpendicular to the fjord-lake axis on the south-eastern margin of the central basin (Figures 3c and 8). The ridge has an asymmetric arcuate shape with a steeper slope facing upstream; this pattern is typical of a morainic deposit (e.g., Cowan et al., 2010; Forwick & Vorren, 2010; Hilbe et al., 2011; Kempf et al., 2013; Hodgson et al., 2014; Batchelor & Dowdeswell, 2015). The sub-bottom profiles also show that the ridge is composed of U1, also suggesting that it is a moraine. Other small transverse ridges (≤700-m long, ≤80-m high) are observed near the lake outlet (Figures 3d and 10), and the sub-bottom profiles also show ice-contact sediments (U1) as a basal unit (Figure 10a). These ridges are interpreted here as morainic sills. The shallow complex topography at the lake outlet is also interpreted as a morainic deposit, forming a sill that separates Grand Lake from Little Lake. Terrestrial moraines are also observed downvalley, forming wide sinuous crests perpendicular to the fjord axis (Figure 11d).

Glacial lineations

The lake is also surrounded by numerous short, elongated crests that form fragmented glacial lineations (500–1000-m long, 100–200-m wide) that vary in their orientation, although most point toward Lake Melville (Figure 11). These glacial lineations also extend west inland far

beyond the head of the fjord of Grand Lake. Larger glacial lineations (>2 km) are also observed north of Lake Melville and are oriented to the north-east (Figure 11e).

The numerous glacial lineations located within a corridor focusing toward the same direction suggest that an ice stream flowed in the area at some point during the last glaciation; such an ice stream has been reported by Margold et al. (2018) in the area (Figure 11c). Topographic troughs, proximal ice calving margins and soft sedimentary beds are key factors that can trigger ice streaming (Winsborrow et al., 2010; Stokes et al., 2016). In this respect, a calving margin in Lake Melville has been suggested previously by Fulton and Hodgson (1979). However, although ice streams are commonly observed in topographic troughs (Winsborrow et al., 2010), there are no apparent topographic controls of the fjord valley on this particular ice stream as it does not follow the same axis as Grand Lake. Only minor lineations focus toward the bay at the Beaver River mouth located at the head of the former fjord.

Central channel

A central channel is observed on the swath bathymetric imagery near the lake outlet. The channel is bordered by many small depositional lobes and is crossed by morainic ridges. The central south-eastern extremity of the channel is aligned with the lake outlet, but it is separated from the outlet by a shallow hummocky moraine. The sub-bottom profiles indicate that the channel existed prior to the deposition of U2 (Figures 3d and 10b,c), as the parallel reflections form a concave depression. Unfortunately, the acoustic attenuation in the sediments prevents determining whether the channel was formed during the deposition of U2 or whether its parallel reflections drape the underlying topography. The existence of buried preglacial fluvial valleys in such fjord environments has been invoked by Lajeunesse (2014), and the central channel at the lake's outlet may be a morphological expression of such an ancient fluvial valley, such as that proposed for another deep fjord-lake in eastern Canada (Gagnon-Poiré et al., 2018). However, since the central channel is observed strictly near morainic ridges, we suggest that its formation is related rather to the erosive proglacial discharge at the ice margin. Such proglacial discharge is heavily loaded with sediments and can form plunging turbidity currents (e.g., Syvitski & Shaw, 1995). Since the retreat of the LIS margin followed the fjord orientation toward a deeper bathymetry, the formation of such a turbidity channel on a positive slope remains possible. The central channel at the lake outlet could be a morphological expression of deglacial turbidity currents delivered at the ice front as the LIS retreated episodically toward the deeper central basin.

DISCUSSION

Deglacial sequence of the fjord

During the Younger Dryas, the LIS margin was positioned at the entrance of Lake Melville, depositing the Little Drunken and Kenamu moraines around 10.2 cal ka BP; these moraines form part of the extensive North Shore morainic complex (King, 1985; Occhietti et al., 2011). The LIS first flowed north-eastward and produced large-scale glacial lineations until the deglacial phase of Lake Melville, when a calving bay established between 10–8 ka BP (Figure 12)., The calving bay accelerated the retreat of the LIS margin in the area of this large water body (Fulton & Hodgson, 1979; Vilks et al., 1987).

The numerous glacial lineations forming an ice stream oriented toward Lake Melville (Figure 11) indicate that: (1) for at least a period of time, ice retreat was controlled by the calving margin of the LIS into Lake Melville; and (2) the deep valley of Grand Lake did not strongly control the pattern of ice retreat since the main ice stream flowed obliquely over the fjord without following the same NE–SW axis. Ice streams have been reported by Stokes et al. (2016) and Margold et al. (2018) on the continental shelf margin of the Labrador Sea and a few hundred kilometres south of Grand Lake. The reported ice stream south of Grand Lake also flowed toward Lake Melville (Figure 11c); however, it followed a S–N direction (Margold et al., 2018; i.e., ice stream #186). The Margold et al. (2018) ice stream #186 presents similar landforms and a small convergent set of well-defined lineations. Based on the isochrones proposed by Dyke (2004) for the LIS retreat, Margold et al. (2018) dated the ice stream at ~9.5 to 8.1 cal ka BP. This date is, however, purely conceptual as no investigations have confirmed its absolute age. The proximal calving bay formed in Lake Melville and the two convergent sets of glacial lineations pointing toward the lake indicate that the ice drainage was directed toward Lake Melville to form ice streams. This reorganisation of the drainage pattern shifting from a north-east orientation to a multidirectional flow pointing toward Lake Melville probably reflects a thinning of the LIS in the area and a greater topographic control of ice flow (Figure 12). Therefore, the large water body of Lake Melville influenced the pattern of ice retreat in eastern Labrador where a calving bay formed and drained the LIS through ice streams despite the orientation of the Grand deep fjord valley. The Younger Dryas cold episode likely generated a positive mass balance of the LIS that enhanced ice stream activity (Stokes and Clarke, 1999; Stokes et al., 2016).

The LIS margin stabilised along the western shore of Lake Melville to form the Sebaskachu moraine 4 km east of the Grand Lake outlet; thus, the fjord remained fully glaciated at that time. Based on shell dates from west of Goose Bay (7.5 ka, GSC-1254) and west of the Sebaskachu moraine (7.6 ka, GSC-2970), the moraine formed prior to 8 cal ka BP (King, 1985; Syvitski & Lee, 1997). The formation of the Sebaskachu moraine probably correlates to the 8.2 cal ka BP cold period recorded in the Greenland ice cores, an event that affected most of the Northern Hemisphere (Fulton & Hodgson, 1979; Occhietti et al., 2011). Ullman et al. (2016) obtained two [10]Be dates (8.6 cal ka BP) 20 km south-west of Grand Lake and 15 km west of the Sebaskachu moraine, also indicating that the Grand Lake area was ice-free at that time (Figure 13). The morainic sills observed on the swath bathymetry imagery and the sub-bottom profiles (U1) indicate that the LIS margin stabilised inside the fjord and that its retreat toward the NW occurred episodically (Figure 13). Including the Sebaskachu moraine, five sublacustrine morainic sills are observed over a distance of only 13 km near the lake outlet. The closely spaced moraines (0.5–3 km) at the lake outlet indicate that the ice margin retreat was punctuated by multiple stabilisations. This shallow sector of the lake likely acted as an anchor point where the ice margin could stabilise. A terrestrial moraine (Figure 13) lacking any sublacustrine section is also observed between the fifth and sixth subaquatic moraines, suggesting that the LIS retreated faster within the fjord than on land. The sixth and final morainic sill lies upstream of a transverse tributary valley on the south-eastern margin of the deep central basin. Ice marginal retreat rates tend to decrease or reach zero when a valley or ice margin narrows as the area available for heat exchange decreases as the glacial ice surface in contact with the marine waters is reduced (Syvitski & Shaw, 1995; Evans, 2003). In Grand Lake, the LIS margin stabilised when ice retreated upstream to a lateral valley, probably during a re-equilibration phase. A tributary glacier flowing from the lateral valley must have disconnected from the main glacier in the fjord valley, narrowing the ice margin and reducing the area available for heat exchange between the glacier and marine waters. Such a re-equilibration phase of a glacier in narrows is well documented by Syvistki & Shaw (1995). No other morainic sills are observed to the north-west as the fjord-lake deepens, indicating that the ice retreated continuously throughout the rest of the basin or became decoupled from the fjord floor and retreated as a floating ice-tongue. However, the acoustic attenuation in the thick sedimentary sequence of the deep central basin prevents observation of the acoustic basement and prevents a determination of whether the glacier was grounded and able to produce glacial morphologies, such as mega-scale glacial lineations. Glacial lineations on fjord floors tend to

get buried by the continuous sedimentation that has occurred since deglaciation (Brouard & Lajeunesse, 2019).

In summary, the morphology of the valley influenced the rates of deglaciation and caused six stabilisations of the ice margin at the fjord outlet and inside the lake. However, the large number of morainic sills over such a short distance and long period, as supported by numerous dates from the literature, suggest that the Sebaskachu moraine is most likely a larger morainic complex formed between 8.6 and 8 cal ka BP (Fulton & Hodgson, 1979; King, 1985; Syvitski & Lee, 1997; Occhietti et al., 2011; Ullman et al., 2016). Such a timeline correlates with the Cockburn morainic complex located on Baffin Island, dated between 9.3–8 cal ka BP and that is also composed of numerous smaller moraines (Briner et al., 2016). Around 8.47 ka, the large ice-damned Lake Agassiz-Ojibway—located along the southern margin of the LIS—drained catastrophically through Hudson Bay and Hudson Straight into the Labrador Sea and Atlantic Ocean (Barber et al., 1999; Lajeunesse & St-Onge, 2008). This freshwater outburst likely triggered the 8.2 cal ka BP cold event (Barber et al., 1999; Teller et al., 2002). Together with the Sakami and Cockburn moraines, both of which culminated around the 8.2 ka event, the Sebaskachu moraine reflects a strong climatic control on LIS deglaciation. The presence of the numerous moraines that form a complex suggest a long interval of ice margin readvance and/or stabilisation, much like for the Cockburn morainic complex. Therefore, both fjord morphology and climate influenced the retreat of the LIS margin at the valley outlet.

As the LIS margin retreated from the fjord, the sea invaded the overdeepened glacial valley and deposited a thick glaciomarine unit (U2a & U2b) over the basal till (U1). In a proglacial environment, sedimentation rates and conditions depend on the proximity of the ice margin in relation to RSL, which controls water depth, meltwater energy and sediment input (Vilks et al., 1987; Syvitski & Lee, 1997). As the LIS margin retreated farther inland, the fjord became gradually isolated from the deglacial sea due to glacio-isostatic rebound to form a deep freshwater-enclosed basin that received paraglacial sediments transported via fluvial discharge (U3). Paraglacial deposits have been observed in fjord-lakes of eastern Quebec (Gagnon-Poiré et al., 2018) and within glacio-isostatically raised deltaic complexes along Quebec's North Shore (Dietrich et al., 2017). These deposits were originally interpreted as deposits related to the retreat of the LIS margin from the watershed, causing a significant reduction of marine delta progradation when sedimentation was limited to the snowmelt discharge of the rivers. Therefore, the formation of the deltas at the Beaver and Naskaupi river mouths likely began

during deglaciation; however, the attenuation of the acoustic signal in the deltaic sediments prevents observation of the base of the deltas. During the paraglacial period, glacial sediments were remobilised from the fluvial valleys with intense fluvial discharge during the snowmelt season transporting a high sediment load. During intense flooding, fluvial inputs of paraglacial sediments likely formed the buried back-stepping beds, located 18 km downstream the modern Naskaupi River mouth. No other evidence of a catastrophic hydrodynamic event, such as a jökulhlaup, has been observed from the same stratigraphic horizon. Normandeau et al. (2019) demonstrated, however, that the retreat pattern of a glacier controls the occurrence of turbidity currents. This suggests that the LIS may have continued to occupy the Grand Lake watershed during the formation of the back-stepping beds in U3a. An outburst flood may have also formed the back-stepping beds, and the beginning of the paraglacial period may not be that clear from the stratigraphic record. The fjord finally disconnected from the sea around 3.2 ka BP (Fizthugh, 1973) to form the fjord-lake. Postglacial sedimentation rates are much lower than the deglacial and paraglacial rates as sediment delivery is now restricted to seasonal fluvial discharge. MMDs and coarse-grained sediments are deposited on the deltas (U3a), whereas the fine-grained sediments are transported and deposited downstream in the fjord (U3b).

Deglacial gullies

The submarine gullies observed in Grand Lake are poorly documented compared to terrestrial gullies, which are defined as erosional landforms formed by a complex interaction of multiple factors, such as lithology, topography, vegetation cover, marine regression (Conforti et al., 2011). However, gullying is also an important component of the sedimentary dynamics of Grand Lake during ice retreat given that 87% of the sublacustrine slopes are covered by a dense network of gullies. The carving in U1 and the overlying drape of the younger U2 indicate that gully formation occurred during deglaciation. Gullies in ice-contact sediments have been observed in fjords and are associated with high proglacial sedimentation rates (Batchelor et al., 2018, Brouard & Lajeunesse, 2019). Such high proglacial deposition rates imply that the discharge is heavily loaded in sediments and can lead to a high erosional capacity.

The position of the gullies relative to the marine limit and the incised sedimentological units is a good indicator of the timing of formation and the erosional process. Gullies incised into a glaciomarine unit (U2) at an elevation between the marine limit and modern lake level suggest a marine regression. Otherwise, gullies located under the modern lake level, carved in ice-contact sediments and conformably draped by younger glaciomarine sediments suggest that the

erosion occurred somewhere between the deposition of the glacial diamicton and the marine regression. Therefore, the gullies most likely formed via the highly erosive, high sediment load proglacial meltwaters. In such a context, the relative position of the gullies in the stratigraphic framework and the deglacial, paraglacial and postglacial water level model can act as proxies for identifying the context of the formation of such erosive landforms. Gully formation in Grand Lake was thus related more to ice-contact sedimentary processes than to a past sea-level lowstand, as observed in other fjords (Overeem & Syvitski, 2010; Van Daele et al., 2016).

Mass-movement deposits (MMDs)

The hummocky morphologies, scarps, depositional lobes and chaotic acoustic facies observed on the swath bathymetry imagery and sub-bottom profiles indicate that Grand Lake has been influenced by gravity-driven processes since deglaciation. Three mechanisms probably triggered these mass movements based on the shape, acoustic properties, stratigraphic position and size of the deposits.

First, remobilisation of surficial sediments from oversteepened slopes deposited small-scale MMDs at the toe of the steep slopes (Hampton et al., 1996; Locat & Lee, 2002; Hilbe et al., 2011; Moernault & De Batist, 2011; Van Daele et al., 2013). Numerous small-scale MMDs located at the toe of steep sidewalls (≤39°) in Grand Lake are present in the sub-bottom profiles with an erosive base and a lens geometry pinching out away from the sidewall and that appear as small lobes on the swath bathymetric imagery. The steepness of the sidewalls (slope ≤39°) does not allow a thick accumulation of sediments as the gravitational force applies a high shear stress leading to eventual slope failure (e.g., Hampton et al., 1996; Fanetti et al., 2008). MMDs are observed at various levels in U2 and U3, revealing multiple slope readjustments over time when the critical stability angle was exceeded. MMDs resulting from slope failure are commonly observed in fjords, which are characterised by steep slopes and high sedimentation rates (Syvitski et al., 1986; Syvitski & Shaw, 1995; Hampton et al., 1996).

Second, a delta collapse must have formed the MMD observed at the fjord head. This MMD covers the entire lake width and is characterised on the acoustic sub-bottom profiles by a hummocky morphology and chaotic internal reflections. The swath bathymetric imagery also shows an extended hummocky topography and headscarps near the Beaver River mouth. In fjords, mass movements near deltas are common (Syvitski & Shaw, 1995; Gilbert & Butler, 2004; Girardclos et al., 2007; Waldmann et al., 2010) as the depositional rates are at a maximum at river mouths. Underconsolidated sediments can produce weak layers prone to

failure (Hampton et al., 1996); therefore, mass movements on the delta of the Beaver River—and the deposition of a large volume and extended MMD—are likely due to the overloading of underconsolidated and rapidly deposited sediments. This delta collapse produced a wider MMD than the abovementioned surficial failures of oversteepened sidewalls.

Finally, a possible earthquake during the rapid glacio-isostatic rebound may have also triggered a large-scale submarine mass movement. The swath bathymetry imagery and sub-bottom profiles show a large-scale MMD along the south-eastern margin of the deep central basin, westward of a large oblique headscarp. Many submarine MMDs are associated with earthquakes when large volumes of sediment and widespread deposits are involved (e.g., Bertrand et al., 2008; Fanetti et al., 2008). On a flat bottom floor, an external force, such as an earthquake, is required to reduce the internal cohesion of soft sediments and generate a failure (Hampton et al., 1996). Rapid initial glacio-isostatic rebound during deglaciation can cause earthquakes in an aseismic region and activate passive geologic faults (Stocker et al., 2010). The position of the MMD on sub-bottom profiles at the limit of U2b and U3 indicates that the mass movement occurred during the transition phase of the fjord as it shifted from a marine to a lacustrine basin. Based on geological map of the area, the headscarp is positioned over a passive fault indicating that the failure was initiated nearby. The closest record of a seismicity (M ≥5) in the region is located 450 km to the north-east at the continental margin of the Labrador Sea (Adams & Basham, 1991). Brooks (2016), however, suggested that seismic activity can increase during deglacial times due to the crustal deformation. Therefore, this mass movement could be of seismic origin during the rapid glacio-isostatic rebound that reactivated a fault because: (1) its deposit is widespread across the lake floor; (2) glacio-isostatic rebound was active during the transition phase from a glaciomarine to a lacustrine basin; and (3) the failure occurred on a nearly flat bottom floor (slope <1°) near a fault. However, there is no evidence of other synchronous mass movements within the Lake Grand stratigraphy. Deglaciation was also characterised by high sedimentation rates, which can also reduce slope stability and produce mass movements (Lajeunesse & Allard, 2002).

Modern sedimentary processes

The analysis of the hydroacoustic dataset collected in Grand Lake suggests that modern sedimentary processes are related to slope dynamics and river sediment supply. The small lobes of MMDs observed in U3 at the toe of the slopes near the lake outlet indicate that slope failures remain part of the modern sedimentary dynamics in Grand Lake. The frequency of slope

failure, however, is currently lower than during deglaciation as deposition rates have decreased sharply relative to the deglacial phase (Syvitski et al., 1986; Syvitski & Shaw, 1995; Gilbert et al., 2006). Similarly, the well-defined sediment waves of the Naskaupi River delta on the swath bathymetric imagery indicate that density flows from river discharge are forming and preserving the bedforms on the bottom floor. However, the sediment waves near the mouth of the Beaver River are subdued on the swath bathymetric imagery relative to the active ones observed near the Naskaupi River. The migration of the Beaver River mouth away from the slope where the main concentration of sediment waves is observed would explain their smooth appearance on the bathymetry as density flows are no longer delivered onto this slope. Older, i.e., early Holocene, sediment waves are therefore slowly becoming buried under a drape of recent sediments; the modern sediment supply, however, is not restricted to the large river mouths at the fjord head as small-scale sediment waves are also observed on small banks where small streams enter the lake (Figure 8).

CONCLUSION

High-resolution swath bathymetry and acoustic sub-bottom profiler data collected from Grand Lake (Labrador) provide new and detailed information related to deglaciation dynamics and Late Quaternary sedimentary processes in a deep fjord-lake located in an aseismic area. The geomorphological map and the stratigraphic framework provided in this paper also offer new insights into regional deglaciation. Glacial lineations observed on a DEM indicate that an ice stream occupied the area during the late-glacial period, most probably during the calving bay phase of Lake Melville. This ice stream flowed toward Lake Melville and was not structurally controlled by the fjord valley of Grand Lake.

The stratigraphic framework of the lake is typical of deglacial sedimentary sequences of eastern Canadian lakes that are located below the marine limit. The presence of morainic sills along the lake axis indicate that deglaciation of Grand Lake and its valley was marked by six stabilisation phases of the LIS margin. The distribution of the morainic sills inside the fjord indicate that deglaciation was structurally controlled in the fjord, and the retreat of the LIS was episodic at the shallow outlet and continuous in the deep central basin. The moraines at the fjord outlet form a morainic complex that was most likely deposited during the 8.2 cal ka BP cold event. The reported stabilisation phase of the LIS margin in Grand Lake during this cold event indicates that regional deglaciation was also climatically controlled.

The swath bathymetric imagery allowed the observation of a dense network of gullies on the lateral slopes of the lake, a network that covers 87% of the sidewalls of the lake. Such submarine gullies have been observed in other fjord settings, but their mechanism of formation remains poorly documented in the literature. The acoustic sub-bottom profiles indicate that the gullies were eroded into ice-contact deposits or bedrock and subsequently draped by a younger glaciomarine unit that preserved the landforms. The erosion in U1 suggests that the gullies were eroded by pulses of highly erosive ice-contact/proximal meltwater discharge on these steep slopes.

Based on the shape, acoustic properties, position and size of the MMDs observed in the lake basin, three different trigger mechanisms were identified for the slope failures: (1) instability of the critically inclined steep, lateral slopes; (2) instability of the delta where sediments continuously accumulate; and (3) a possible earthquake. The presence of MMD lenses at various levels in the acoustic stratigraphy suggests that slope failures occurred during all time periods and should be considered as an active sedimentary process in this fjord-lake today. Nonetheless, postglacial sedimentation rates normally tend to be much lower than deglacial sedimentation rates (Syvitski et al., 1986; Syvitski & Shaw, 1995; Gilbert et al., 2006), which suggests a decrease in the recurrence of gravity-driven processes.

The geomorphology of Grand Lake is inherited mainly by the last glaciation and deglaciation, as modern sedimentary processes form only small-scale morphologies on the lake floor compared to the larger-scale deglacial landforms that include gully networks, morainic sills and a possible seismically induced MMD.

ACKNOWLEDGMENTS

REFERENCES

Aarseth, I. (1997). Western Norwegian fjord sediments: age, volume, stratigraphy, and role as temporary depository during glacial cycles. *Marine Geology*, *143*(1-4), 39-53.

Adams, J. & Basham P. (1991) The seismicity and seismotectonics of Canada east of the Cordillera. *Geoscience Canada*, *16*(1), 3-16

Andrews, J. T., Keigwin, L., Hall, F., & Jennings, A. E. (1999) Abrupt deglaciation events and Holocene palaeoceanography from high-resolution cores, Cartwright Saddle, Labrador Shelf, Canada. *Journal of Quaternary Science*, *14*(5), 383-397

Baeten, N. J., Forwick, M., Vogt, C., & Vorren, T. O. (2010). Late Weichselian and Holocene sedimentary environments and glacial activity in Billefjorden, Svalbard. *Geological Society, London, Special Publications*, *344*(1), 207-223.

Ballantyne, C. K. (2002) Paraglacial geomorphology. *Quaternary Science Reviews, 21*, 1935-2017

Barber, D. C., Dyke, A., Hillaire-Marcel, C., Jennings, A. E., Andrews, J. T., Kerwin, M. W., Bilodeau, G., McNeely, R., Southons, J., Morehead, M. D., & Gagnon, J. M. (1999). Forcing of the cold event of 8,200 years ago by catastrophic drainage of Laurentide lakes. *Nature*, *400*(6742), 344-348.

Batchelor, C. L., & Dowdeswell, J. A. (2015). Ice-sheet grounding-zone wedges (GZWs) on high-latitude continental margins. *Marine Geology*, *363*, 65-92.

Batchelor, C. L., Dowdeswell, J. A., & Rignot, E. (2018). Submarine landforms reveal varying rates and styles of deglaciation in North-West Greenland fjords. *Marine Geology*, *402*, 60-80.

Beck, C., Manalt, F., Chapron, E., Van Rensbergen, P., & De Batist, M. (1996) Enhanced seismicity in the early post-glacial period: evidence from the post-Würm sediments of Lake Annecy, Northwestern Alps. *Journal of Geodynamics*, *22*(1/2), 155-171

Bertrand, S., Charlet, F., Chapron, E., Fagel, N., & De Batist, M. (2008) Reconstruction of the Holocene seismotectonic activity of the Southern Andes from seismites recorded in Lago Icalma, Chile. *Palaeogeography, Palaeoclimatology, Palaeoecology*, *259*, 301-322

Blake Jr, W. (1956). Landforms and topography of the Lake Melville area, Labrador, Newfoundland. *Canada Department of Mines and Technical Surveys Geographical Bulletin*, *9*, 93-97.

Briner, J. P., McKay, N. P., Axford, Y., Bennike, O., Bradley, R. S., de Vernal, A., & Jennings, A. (2016). Holocene climate change in Arctic Canada and Greenland. *Quaternary Science Reviews*, *147*, 340-364.

Brooks, G. R. (2016). Evidence of late glacial paleoseismicity from submarine landslide deposits within Lac Dasserat, northwestern Quebec, Canada. *Quaternary research*, *86*(2), 184-199

Brouard, E., & Lajeunesse, P. (2019). Glacial to postglacial submarine landform assemblages in fiords of northeastern Baffin Island. *Geomorphology*, *330*, 40-56.

Boyd, B. L., Anderson, J. B., Wellner, J. S., & Fernandez, R. A. (2008). The sedimentary record of glacial retreat, Marinelli Fjord, Patagonia: Regional correlations and climate ties. *Marine Geology*, *255*(3), 165-178.

Clarke, J. E. H., Marques, C. R. V., & Pratomo, D. (2014). Imaging active mass-wasting and sediment flows on a fjord delta, Squamish, British Columbia. In *Submarine Mass Movements and Their Consequences* (pp. 249-260). Springer, Cham.

Church, M., & Ryder, J. M. (1972) Paraglacial sedimentation: A consideration of fluvial processes conditioned by glaciation. *Geological Society of America Bulletin, 83*, 3059-3072

Conforti, M., Aucelli, P. P., Robustelli, G., & Scarciglia, F. (2011). Geomorphology and GIS analysis for mapping gully erosion susceptibility in the Turbolo stream catchment (Northern Calabria, Italy). *Natural Hazards*, *56*(3), 881-898.

Cowan, E. A., Seramur, K. C., Powell, R. D., Willems, B. A., Gulick, S. P., & Jaeger, J. M. (2010). Fjords as temporary sediment traps: History of glacial erosion and deposition in Muir Inlet, Glacier Bay National Park, southeastern Alaska. *Geological Society of America Bulletin*, *122*(7-8), 1067-1080.

Department of Natural Resources, Government of Newfoundland and Labrador. Geoscience Online: https://gis.geosurv.gov.nl.ca/

Desloges, J. R., & Gilbert, R. (1998). Sedimentation in Chilko Lake: a record of the geomorphic environment of the eastern Coast Mountains of British Columbia, Canada. *Geomorphology*, *25*(1), 75-91.

Dietrich, P., Ghienne, J. F., Normandeau, A., & Lajeunesse, P. (2017). Reconstructing ice-margin retreat using delta morphostratigraphy. *Scientific Reports*, *7*(1), 16936.

Dowdeswell, J. A., Canals, M., Jakobsson, M., Todd, B. J., Dowdeswell, E. K., & Hogan, K. A. (2016). The variety and distribution of submarine glacial landforms and implications for ice-sheet reconstruction. *Geological Society, London, Memoirs*, *46*(1), 519-552.

Dowdeswell, J. A., & Vásquez, M. (2013). Submarine landforms in the fjords of southern Chile: implications for glacimarine processes and sedimentation in a mild glacier-influenced environment. *Quaternary Science Reviews*, *64*, 1-19.

Dyke, A. S. (2004). An outline of North American deglaciation with emphasis on central and northern Canada. *Quaternary Glaciations: Extent and Chronology*, *2*, 373-424.

Elverhøi, A., Lønne, Ø., & Seland, R. (1983). Glaciomarine sedimentation in a modern fjord environment, Spitsbergen. *Polar Research*, *1*(2), 127-150.Evans, D.J.A. (2003) *Glacial Landsystems*. Arnold Edition, London: 532 p.

Eyles, N., Mullins, H. T., & Hine, A. C. (1990). Thick and fast: sedimentation in a Pleistocene fiord lake of British Columbia, Canada. *Geology*, *18*(11), 1153-1157.

Eyles, N., Mullins, H. T., & Hine, A. C. (1991). The seismic stratigraphy of Okanagan Lake, British Columbia; a record of rapid deglaciation in a deep 'fiord-lake' basin. *Sedimentary Geology*, *73*(1-2), 13-41.

Fanetti, D., Anselmetti, F. S., Chapron, E., Sturm, M., & Vezzoli, L. (2008) Megaturbidite deposits in the Holocene basin fill of Lake Coo (Southern Alps, Italy). *Palaeogeography, Palaeoclimatology, Palaeoecology*, *259*, 323-340.

Fitzhugh, W. (1973). Environmental approaches to the prehistory of the North. *Journal of the Washington Academy of Sciences*, *63*(2), 39-53.

Forwick, M., & Vorren, T. O. (2011). Stratigraphy and deglaciation of the Isfjorden area, Spitsbergen. *Norwegian Journal of Geology/Norsk Geologisk Forening*, *90*(4), 163-179.

Forwick, M., Vorren, T.O., Hald, M., Korsun, S., Roh, Y., Vogt, C., & Yoo, K-C. (2010) Spatial and temporal influence of glaciers and rivers on the sedimentary environment in Sassenfjorden and Tempelfjorden, Spitsbergen. *In*: Howe, J. A., Austin, W. E. N., Forwick, M., Paetzel, M. (2010) *Fjords systems and archives*. Geological Society, London, Special Publications, *344*, 163-193

Fulton, R. J., & Hodgson, D. A. (1979). Wisconsin glacial retreat, southern Labrador. *Current Research, Part C, Geological Survey of Canada, Paper*, *79*, 17-21.

Fulton, R. J. (1986) Quaternary Geology of Canada and Greenland. Geological Survey of Canada, *1*, 846 p.

Gagnon-Poiré, A., Lajeunesse, P., Normandeau, A., Francus, P., St-Onge, G., & Nzekwe, O. (2018) Late-Quaternary glacial to postglacial sedimentation in three adjacent fjord-lakes of the Québec North Shore (eastern Canadian Shield). *Quaternary Science Reviews, 186*, 91-110

Gilbert, R., & Butler, R. D. (2004). The physical limnology and sedimentology of Meziadin Lake, northern British Columbia, Canada. *Arctic, Antarctic, and Alpine Research*, *36*(1), 33-41.

Gilbert, R., Crookshanks, S., Hodder, K. R., Spagnol, J., & Stull, R. B. (2006). The record of an extreme flood in the sediments of montane Lillooet Lake, British Columbia: implications for paleoenvironmental assessment. *Journal of Paleolimnology*, *35*(4), 737-745.

Girardclos, S., Schmidt, O. T., Sturm, M., Ariztegui, D., Pugin, A., & Anselmetti, F. S. (2007). The 1996 AD delta collapse and large turbidite in Lake Brienz. *Marine Geology*, *241*(1), 137-154.

Glasser, N. F., & Ghiglione, M. C. (2009). Structural, tectonic and glaciological controls on the evolution of fjord landscapes. *Geomorphology*, 105(3), 291-302.

Green, B. A. (1974) An Outline of the Geology of Labrador. *Geoscience Canada*, *1*(3), 36-40.

Hampton, M. A., Lee, H. J., & Locat, J. (1996) Submarine landslides. *Reviews of Geophysics*, *34*(1), 33-59.

Hansen, L., L'Heureux, J. S., Sauvin, G., Polom, U., Lecomte, I., Vanneste, M. & Krawczyk, C. M. (2013). Effects of mass-wasting on the stratigraphic architecture of a fjord-valley fill: Correlation of onshore, shear-wave seismic and marine seismic data at Trondheim, Norway. *Sedimentary Geology*, *289*, 1-18.

Heirman, K., De Batist, M., Arnaud, F., & De Beaulieu, J. L. (2012). Seismic stratigraphy of the late Quaternary sedimentary infill of Lac d'Armor (Kerguelen archipelago): a record of glacier retreat, sedimentary mass wasting and southern Westerly intensification. *Antarctic Science*, *24*(6), 608-618.

Hilbe, M & Anselmetti, F. S. (2014) Signature of slope failures and river-delta collapses in a perialpine lake (Lake Lucerne, Switzerland). *Sedimentology*, *61*, 1883-1907

Hilbe, M., Anselmetti, F. S., Eilertsen, R. S., Hansen, L., & Wildi, W. (2011) Subaqueous morphology of Lake Lucerne (Central Switzerland): implications for mass movements and glacial history. *Swiss Journal of Geosciences*, *104*, 425-443

Hjelstuen, B. O., Haflidason, H., Sejrup, H. P., & Lyså, A. (2009). Sedimentary processes and depositional environments in glaciated fjord systems—Evidence from Nordfjord, Norway. *Marine Geology*, *258*(1-4), 88-99.

Hjelstuen, B. O., Kjennbakken, H., Bleikli, V., Ersland, R. A., Kvilhaug, S., Euler, C., & Alvheim, S. (2013). Fjord stratigraphy and processes–evidence from the NE Atlantic Fensfjorden system. *Journal of Quaternary Science*, *28*(4), 421-432.

Hodgson, D. A., Graham, A. G., Griffiths, H. J., Roberts, S. J., Cofaigh, C. Ó., Bentley, M. J., & Evans, D. J. (2014). Glacial history of sub-Antarctic South Georgia based on the submarine geomorphology of its fjords. *Quaternary Science Reviews*, *89*, 129-147.

Howe, J. A., Austin, W. E., Forwick, M., Paetzel, M., Harland, R., & Cage, A. G. (2010). Fjord systems and archives: a review. *Geological Society, London, Special Publications*, *344*(1), 5-15.

Josenhans, H. W., Zevenhuizen, J., & Klassen, R. A. (1986) The Quaternary geology of the Labrador Shelf. *Canadian Journal of Earth Sciences*, *23*, 1190-1213

Kempf, P., Forwick, M., Laberg, J. S., & Vorren, T. O. (2013). Late Weichselian and Holocene sedimentary palaeoenvironment and glacial activity in the high-arctic van Keulenfjorden, Spitsbergen. *The Holocene*, *23*(11), 1607-1618.

King, G.A. (1985) A standard method for evaluating radiocarbon dates of local deglaciation: application to the deglaciation history of southern Labrador and adjacent Québec. *Géographie physique et Quaternaire*, *39*(2): 163-182

Lajeunesse, P. (2014). Buried preglacial fluvial gorges and valleys preserved through Quaternary glaciations beneath the eastern Laurentide Ice Sheet. *Geological Society of America Bulletin*, *126*(3-4), 447-458.

Lajeunesse, P., & Allard, M. (2002). Sedimentology of an ice-contact glaciomarine fan complex, Nastapoka Hills, eastern Hudson Bay, northern Québec. *Sedimentary Geology*, *152*(3-4), 201-220.

Lajeunesse, P., Sinkunas, B., Morissette, A., Normandeau, A., Joyal, G., St-Onge, G., & Locat, J. (2017) Large-scale seismically-induced mass-movements in a former glacial lake basin: Lake Témiscouata, northeastern Appalachians (eastern Canada). *Marine Geology*, *384*, 120-130.

Lajeunesse, P., & St-Onge, G. (2008). The subglacial origin of the Lake Agassiz–Ojibway final outburst flood. *Nature Geoscience*, *1*(3), 184.

Locat, J., & Lee, H. J. (2002) Submarine landslides: advances and challenges. *Canadian Geotechnical Journal, 39*(1), 193-212.

Lucas, S. B., & St-Onge, M. R. (Eds.). (1998). *Geology of the Precambrian Superior and Grenville Provinces and Precambrian fossils in North America*. Geological Society of America.

Margold, M., Stokes, C. R., & Clark, C. D. (2018). Reconciling records of ice streaming and ice margin retreat to produce a palaeogeographic reconstruction of the deglaciation of the Laurentide Ice Sheet. *Quaternary Science Reviews*, *189*, 1-30.

Moernaut, J., & De Batist, M. (2011) Frontal emplacement and mobility of sublacustrine landslides: Results from morphometric and seismostratigraphic analysis. *Marine Geology*, *285*, 29-45

Mullins, H. T., & Hinchey, E. J. (1989). Erosion and infill of New York Finger Lakes: Implications for Laurentide ice sheet deglaciation. *Geology*, *17*(7), 622-625.

Mullins, H. T., & Halfman, J. D. (2001). High-resolution seismic reflection evidence for middle Holocene environmental change, Owasco Lake, New York. *Quaternary Research*, *55*(3), 322-331.

Normandeau, A., Lajeunesse, P., & Philibert, G. (2013) Late-Quaternary morphostratigraphy of Lake St-Joseph (southeastern Canadian Shield) : Evolution from a semi-enclosed glacimarine basin to a postglacial lake. *Sedimentary Geology, 295*, 38-52

Normandeau, A., Lajeunesse, P., Gagnon-Poiré, A., & Francus, P. (2016) Morphological expression of bedforms formed by supercritical sediment density flows in four fjord-lake deltas of the south-eastern Canadian Shield (Eastern Canada). *Sedimentology*, 63, 2106-2129

Normandeau, A., Lajeunesse, P., Trottier, A. P., Poiré, A. G., & Pienitz, R. (2017). Sedimentation in isolated glaciomarine embayments during glacio-isostatically induced relative sea level fall (northern Champlain Sea basin). *Canadian Journal of Earth Sciences*, *54*(10), 1049-1062.

Normandeau, A., Dietrich, P., Hughes Clarke, J., Van Wychen, W., Lajeunesse, P., Burgess, D., & Ghienne, J. F. (2019). Retreat pattern of glaciers controls the occurrence of turbidity currents on high-latitude fjord deltas (eastern Baffin Island). *Journal of Geophysical Research: Earth Surface*.

Ó Cofaigh, C. (1998). Geomorphic and sedimentary signatures of early Holocene deglaciation in High Arctic fiords, Ellesmere Island, Canada: implications for deglacial ice dynamics and thermal regime. *Canadian Journal of Earth Sciences*, *35*(4), 437-452.

Occhietti, S., Parent, M., Lajeunesse, P., Robert, F., & Govare, E. (2011) Late Pleistocene – Early Holocene decay of the Laurentide Ice Sheet in Québec-Labrador. In: Ehlers, J., Gibbard, P. L. (Eds.), *Quaternary Glaciations – Extent and Chronology: Part IV: A closer look. Developments in Quaternary Science 15*, 601-630.

Overeem, I., & Syvitski, J. P. M. (2010) Experimental exploration of the stratigraphy of fjords fed by glaciofluvial systems. *In*: Howe, J. A., Austin, W. E. N., Forwick, M., Paetzel, M. (2010) *Fjords Systems and Archives*. Geological Society, London, Special Publications, *344*, 125-142

Peltier, W. R. (2004). Global glacial isostasy and the surface of the ice-age Earth: the ICE-5G (VM2) model and GRACE. *Annual Reviews of Earth Planet Sciences*, *32*, 111-149.

Peltier, W. R., Drummond, R., & Argus, D. F. (2016). The ICE-6G_C (VM5a) global model of the GIA process: Antarctica at high spatial resolution. In *AGU Fall Meeting Abstracts*.

Praet, N., Moernaut, J., Van Daele, M., Boes, E., Haeussler, P. J., Strupler, M., Schmidt, S., Loso, M. G., & De Batist, M. (2016) Paleoseismic potential of sublacustrine landslide records in a high-seismicity setting (south-central Alaska). *Marine Geology*, *384*, 103-119.

Stocker, M. S., Bradwell, T., Howe, J. A., Wilkinson, I. P., & McIntyre, K. (2009). Late glacial ice-cap dynamics in NW Scotland: evidence from the fjords of the Summer Isles region. *Quaternary Science Reviews*, *28*(27), 3161-3184.

Stocker, M. S., Wilson, C. R., Howe, J.A., Bradwell, T., & Long, D. (2010) Paraglacial slope instability in Scottish fjords: examples from Little Loch Broom, NW Scotland. *In*: Howe, J. A., Austin, W. E. N., Forwick, & M., Paetzel, M. (2010) *Fjords Systems and Archives*. Geological Society, London, Special Publications, *344*, 225-242

Stokes, C. R., & Clark, C. D. (1999). Geomorphological criteria for identifying Pleistocene ice streams. *Annals of Glaciology*, *28*, 67-74.

Stokes, C. R., Margold, M., Clark, C. D., & Tarasov, L. (2016). Ice stream activity scaled to ice sheet volume during Laurentide Ice Sheet deglaciation. *Nature*, *530*(7590), 322.

Symons, W. O., Sumner, E. J., Talling, P. J., Cartigny, M. J., & Clare, M. A. (2016). Large-scale sediment waves and scours on the modern seafloor and their implications for the prevalence of supercritical flows. *Marine Geology*, *371*, 130-148.

Syvitski, J. P. (1989). On the deposition of sediment within glacier-influenced fjords: oceanographic controls. *Marine Geology*, *85*(2-4), 301-329.

Syvitski, J. P. (1991). Towards an understanding of sediment deposition on glaciated continental shelves. *Continental Shelf Research*, *11*(8-10), 897-937

Syvitski, J. P. M., Burrell, D. C., & Skei, J. M. (1986) Fjords, processes and products. Springer-Verlag New-York Inc., 379 p.

Syvitski, J. P. M. & Praeg., D.B. (1989) Quaternary sedimentation in the St. Lawrence estuary and adjoining areas, eastern Canada: an overview based on high resolution seismo-stratigraphy. *Géographie physique et Quaternaire, 43*, 291-310

Syvitski, J. P. M., & Lee, H. J. (1997) Postglacial sequence stratigraphy of Lake Melville, Labrador. *Marine Geology*, *143*, 55-79

Syvitski, J. P., & Schafer, C. T. (1996). Evidence for an earthquake-triggered basin collapse in Saguenay Fjord, Canada. *Sedimentary Geology*, *104*(1-4), 127-153.

Syvitski, J. P. M., & Shaw, J. (1995) Sedimentology and geomorphology of fjords. Geomorphology and Sedimentology of Estuaries, *Developments in Sedimentology*, *53*, 113-178

Teller, J. T., Leverington, D. W., & Mann, J. D. (2002). Freshwater outbursts to the oceans from glacial Lake Agassiz and their role in climate change during the last deglaciation. *Quaternary Science Reviews*, *21*(8-9), 879-887.

Trottier, A. P., Lajeunesse, P., Normandeau, A., & Gagnon-Poiré, A. (2018). Deglacial and postglacial paleoseismological archives in mass-movement deposits of lakes of south-central Québec. *Canadian Journal of Earth Sciences*, *56*(1), 60-76.

Turner, A. J., Woodward, J., Dunning, S. A., Shine, A. J., Stokes, C. R., & Cofaigh, C. Ó. (2012). Geophysical surveys of the sediments of Loch Ness, Scotland: Implications for the deglaciation of the Moray Firth Ice Stream, British–Irish ice sheet. *Journal of Quaternary Science*, *27*(2), 221-232.

Ullman, D. J., Carlson, A. E., Hostetler, S. W., Clark, P. U., Cuzzone, J., Milne, G. A., ... & Caffee, M. (2016). Final Laurentide ice-sheet deglaciation and Holocene climate-sea level change. *Quaternary Science Reviews*, *152*, 49-59.

Van Daele, M., Versteeg, W., Pino, M., Urrutia, R., & De Batist, M. (2013). Widespread deformation of basin-plain sediments in Aysén fjord (Chile) due to impact by earthquake-triggered, onshore-generated mass movements. *Marine Geology*, *337*, 67-79.

Van Rensbergen, P., De Batist, M., Beck, C., & Manalt, F. (1998). High-resolution seismic stratigraphy of late Quaternary fill of Lake Annecy (northwestern Alps): evolution from glacial to interglacial sedimentary processes. *Sedimentary Geology*, *117*(1-2), 71-96.

Vilks, G., Deonarine, B., & Winters, G. (1987) L*ate Quaternary Marine Geology of Lake Melville, Labrador*. Geological Survey of Canada, 55 p.

Waldmann, N., Ariztegui, D., Anselmetti, F. S., Coronato, A., & Austin, J. A. (2010). Geophysical evidence of multiple glacier advances in Lago Fagnano (54° S), southernmost Patagonia. *Quaternary Science Reviews*, *29*(9), 1188-1200.

Wardle, R. J., Gower, C. F., Ryan, B., Nunn, G. A. G., James, D.T., & Kerr, A., (1997). *Geological Map of Labrador; 1:1 million scale*. Government of Newfoundland and Labrador, Department of Mines and Energy, Geological Survey, Map 97-07

Winsborrow, M. C., Clark, C. D., & Stokes, C. R. (2010). What controls the location of ice streams? *Earth-Science Reviews, 103*(1-2), 45-59.

Wynn, R. B., Piper, D. J. W., & Gee, M. J. R. (2002) Generation and migration of coarse-grained sediment waves in turbidity current channels and channel-lobe transition zones. *Marine Geology*, *192*, 59-78

Figure 1: Location map of Grand Lake in the eastern Canadian Shield and its paleoenvironmental context around 8.45 ka. Red lines show the Cockburn morainic complex (CMC) on Baffin Island and the Sebaskachu moraine near Grand Lake. The extension of the Laurentide Ice Sheet (LIS) and Glacial Lake Agassiz-Ojibway are from Dyke (2004).
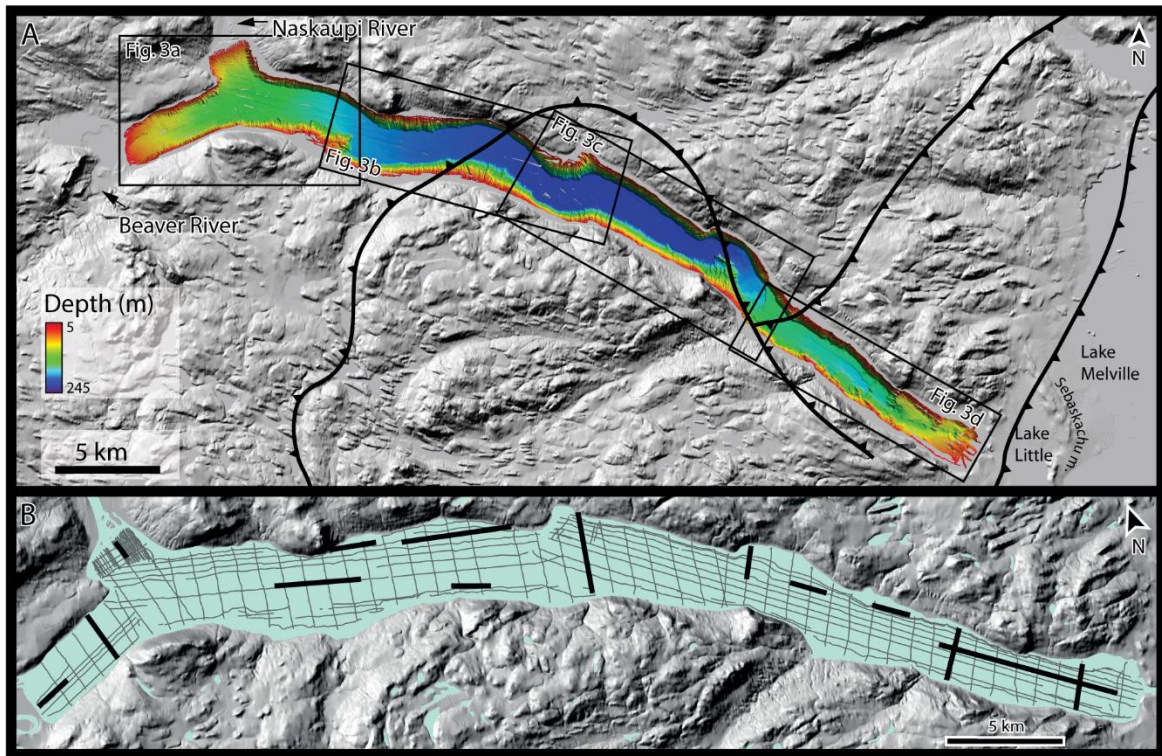
Figure 2: (a) High-resolution swath bathymetric map of Grand Lake. Dotted black lines represent geological faults formed during the Grenville Orogen (Green, 1974). Note the Sebaskachu moraine (~ 8.45 cal. ka) located 4 km downstream of the lake outlet. (b) Profiling survey pattern of the acoustic sub-bottom profiles were acquired using a Knudsen 3212 (3.5 kHz). Dark lines show the profiles presented in this paper. Note that survey lines were run perpendicular to each other to better visualise the distribution of the acoustic units within the lake basin.
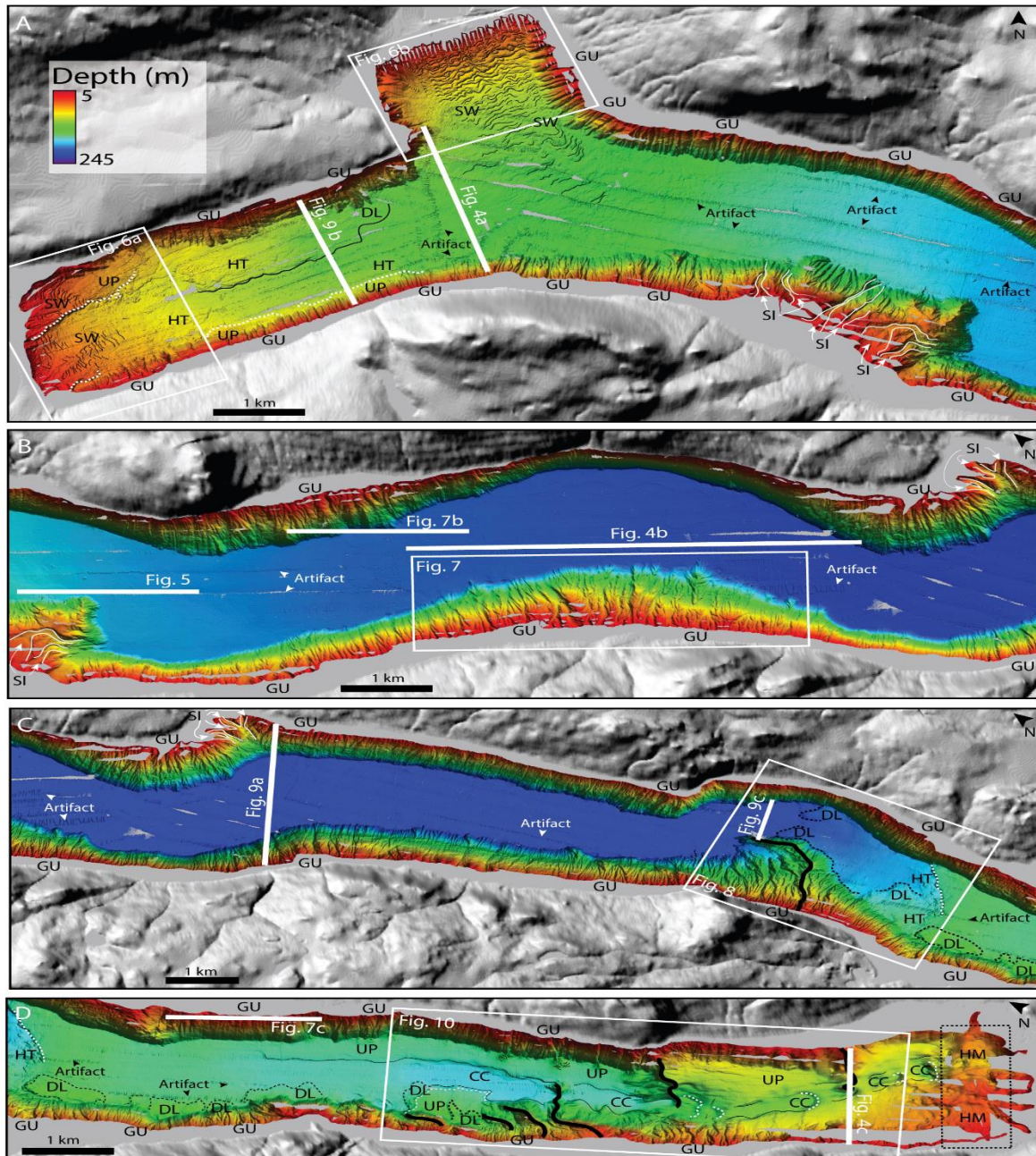
Figure 3: Swath bathymetry images showing the sublacustrine geomorphology of Grand Lake. The white dashed lines represent mass-movement scarps, and the black dashed lines represent the extent of the depositional lobes. SW: sediment waves; HT: hummocky topography; UP: undisturbed plateau; GU: gullies; SI: stream input; DL: deposited lobes; CC: central channel. Morainic sills are shown by bold black lines and hummocky moraine (HM) is represented by the dashed black frame.
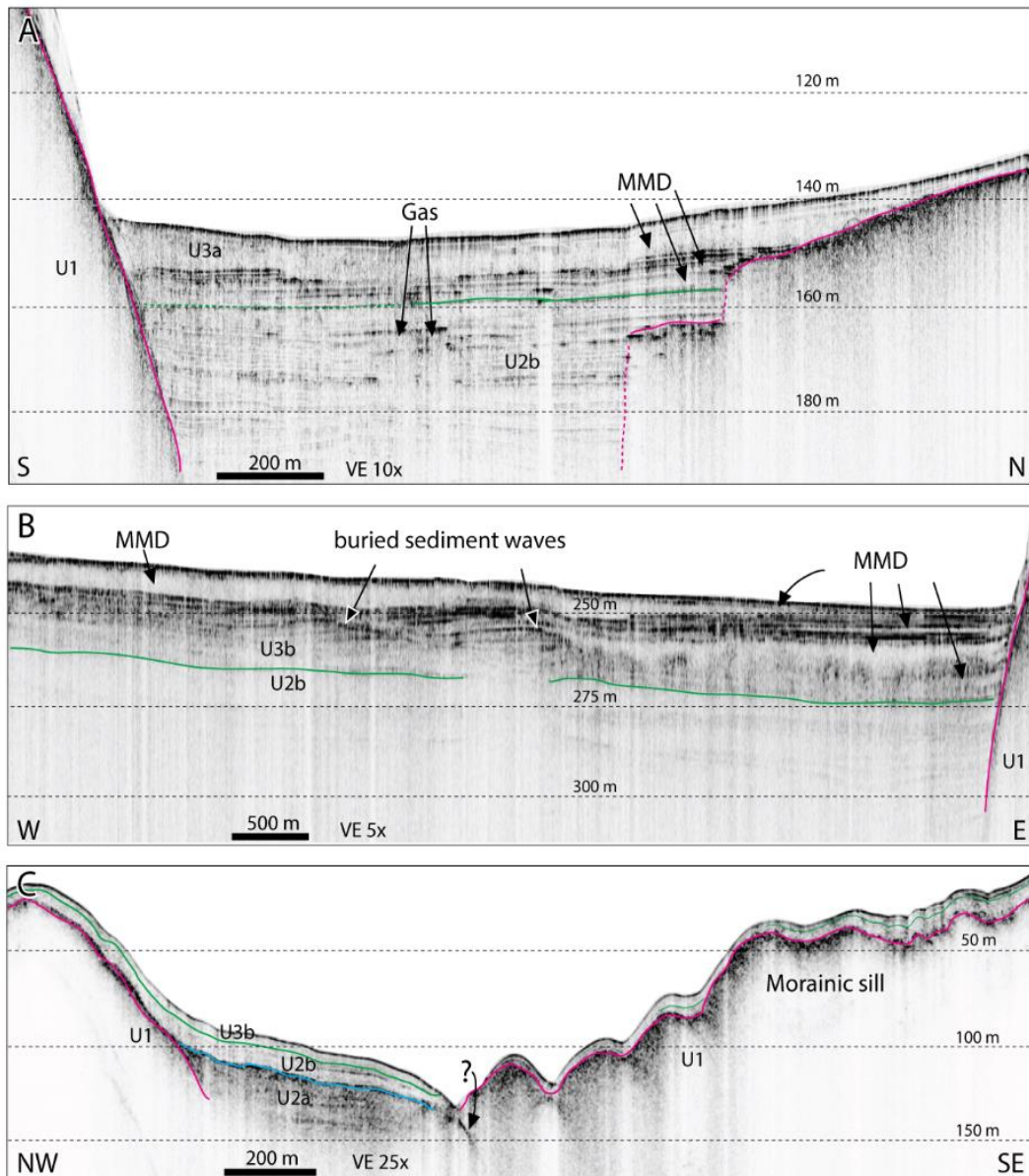
Figure 4: Acoustic sub-bottom profiles showing: the filling of the deep trough by glaciomarine sediments (U2b) at the fjord head (Profile A); buried sediment waves in paraglacial sediments (U3a) in the deep central basin (Profile B); and a morainic sill near the fjord outlet (Profile C). Note that in Profile C, the cross-cutting relationship between U1 and U2a is unclear. Sedimentation rates are lower within the fjord axis with thicker units at the fjord head and thinner units at the fjord outlet. MMD: mass-movement deposits.
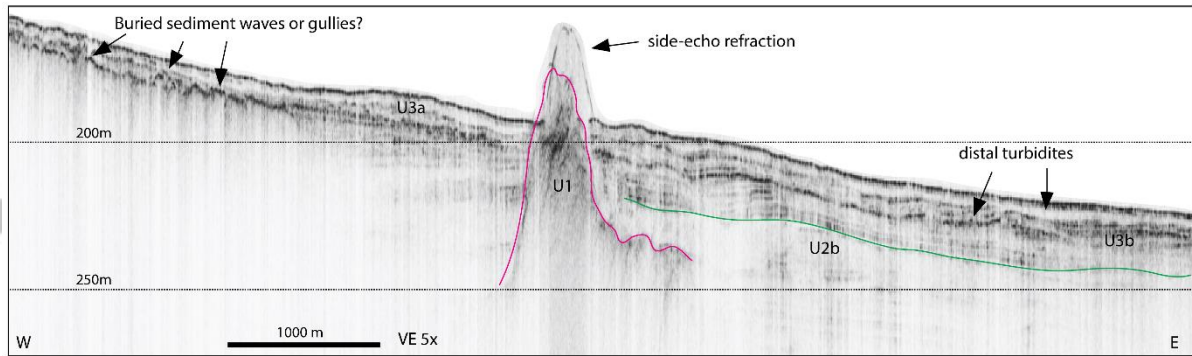
Figure 5: Acoustic profile showing the transition from U3a to U3b away from the river mouth. As the profile is located near the sidewall, it is unclear if the buried undulations observed on the upper slope (U3a) are sediment waves from the Naskaupi River delta or distal gullies from the sidewalls. Note that the acoustic penetration increases away from the river mouth (from west to east) and stacked distal turbidites that form U3b are observed in the central basin. Refer to Figure 3b for the location of the profile. Note that side-echo refraction from the steep sidewalls is observed over U1.
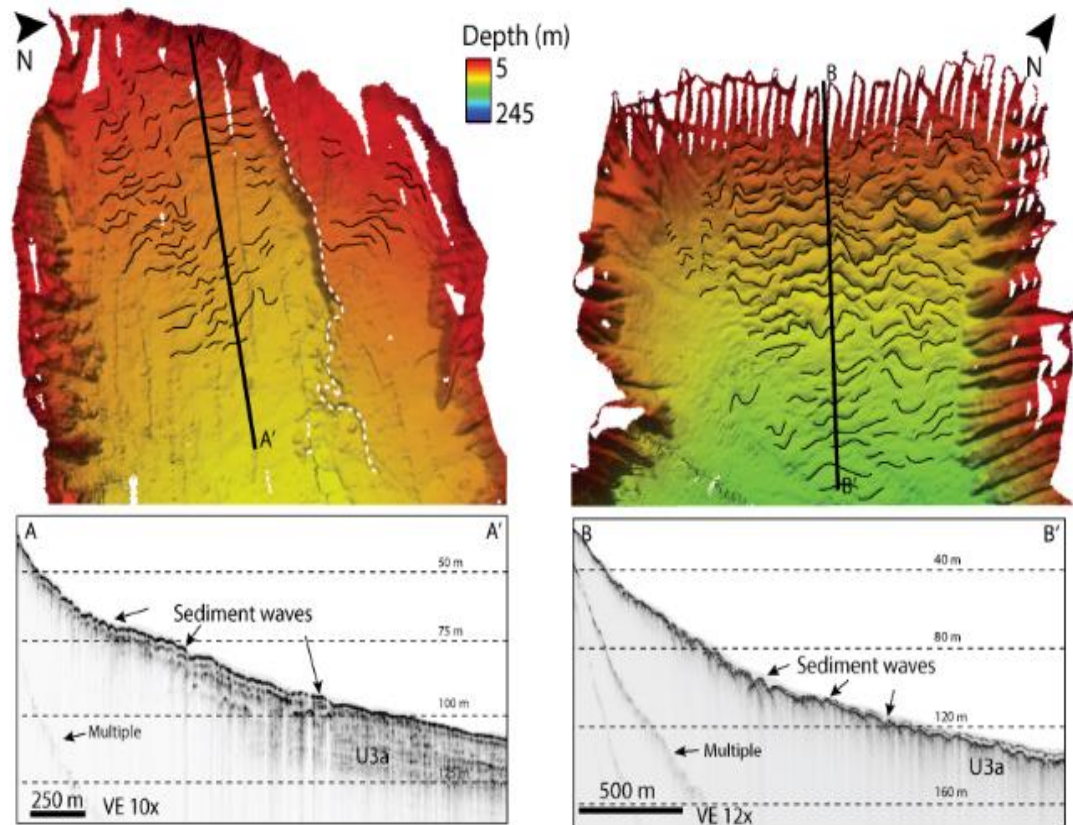
Figure 6: Three-dimensional view of the high-resolution swath bathymetry of the deltas at the Beaver (A) and Naskaupi (B) river mouths illustrating the sediment waves on their frontal slopes. The acoustic sub-bottom profiles present the recent deltaic sediments (U3a) having a greater acoustic penetration away from the river mouth. For the Beaver River delta, the white dashed line on the multibeam bathymetry image represents a mass-movement scarp.
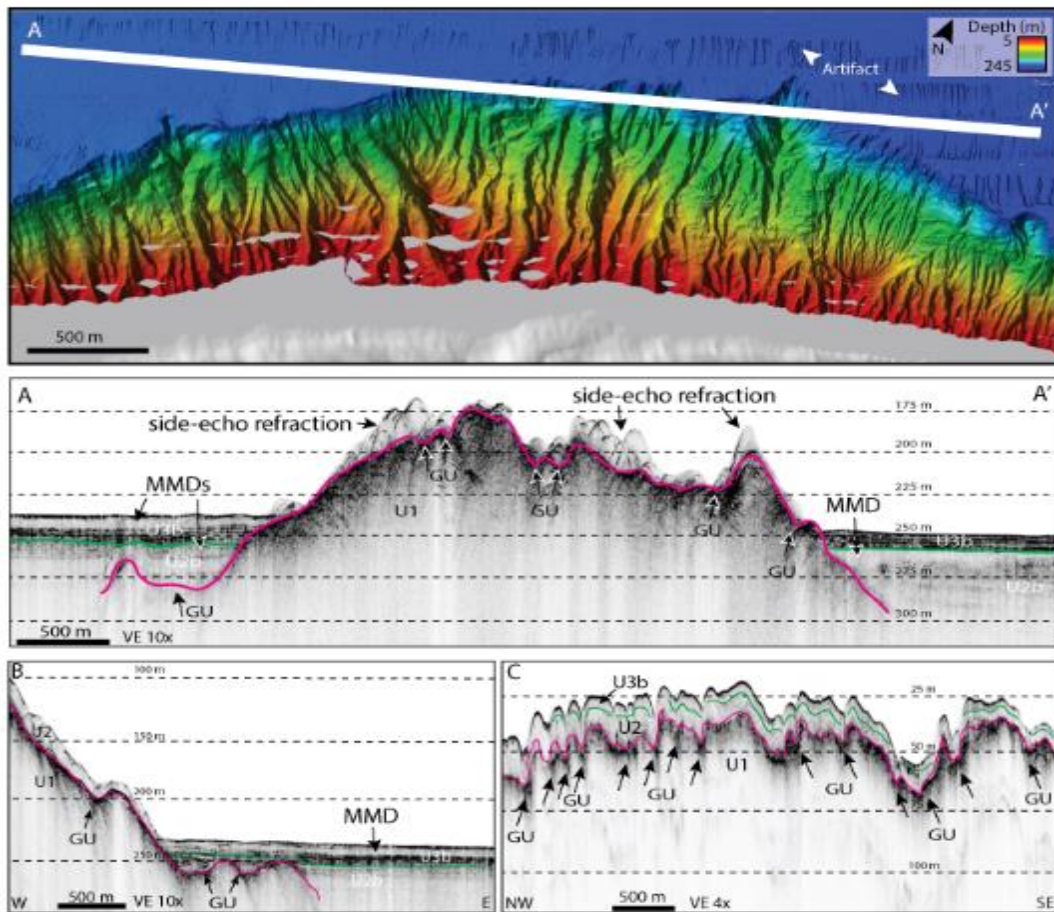
Figure 7: Swath bathymetry image and acoustic sub-bottom profiles showing the dense network of gullies on the steep sidewalls of Grand Lake. Acoustic sub-bottom profiles illustrate that gullies were carved in U1. Profiles A and B show that the base of the gullies that reach the deep central basin are buried under the glaciomarine unit (U2) and mass-movement deposits (MMD). Note that in Profile A, the acoustically transparent unit showing internal hyperboles over U1 is interpreted as a side-echo refraction from the steep rocky sidewalls. Profile C demonstrates that the shallow sections of the gullies were conformably draped by U2 and U3. Refer to Figure 3b for the location of profiles B and C.
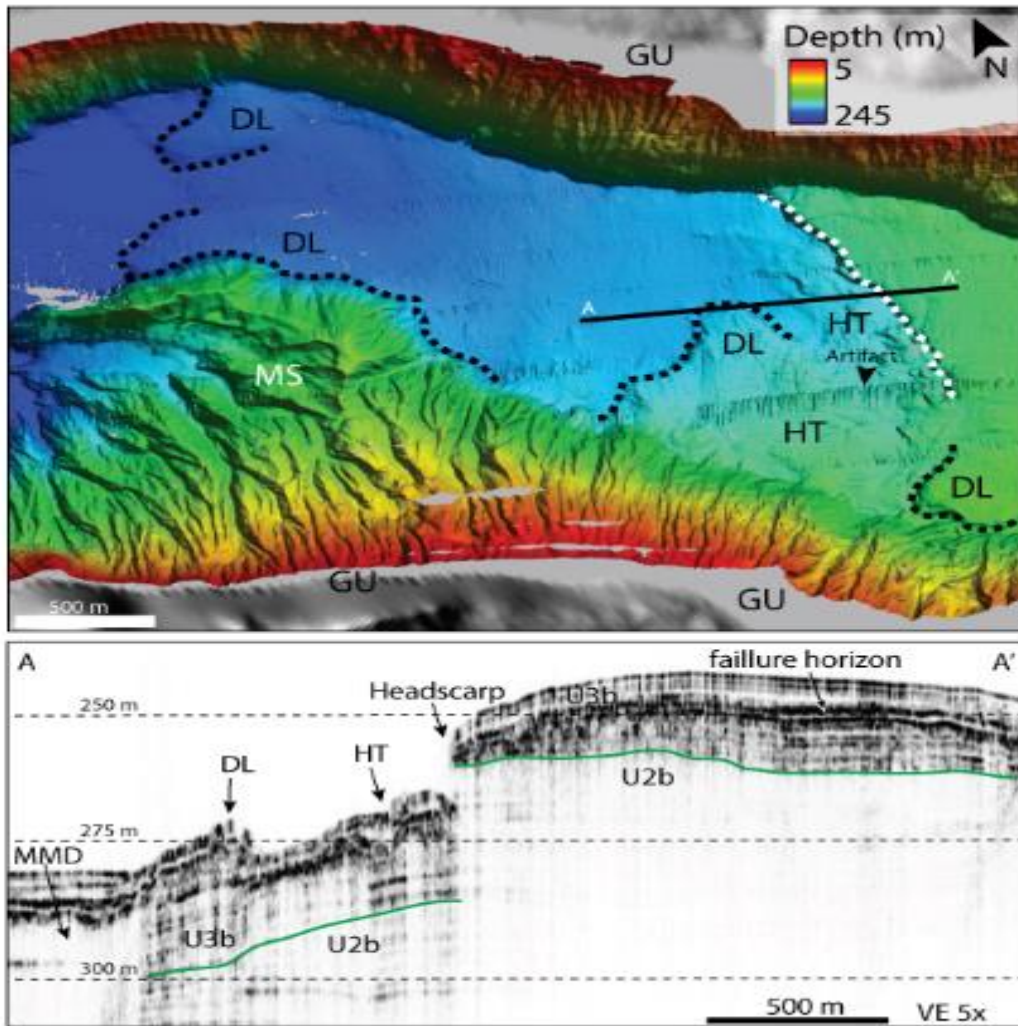
Figure 8: Swath bathymetry image and an acoustic sub-bottom profile showing the widespread MMD along the south-eastern margin of the central basin. On the bathymetric image, a white dashed line represents the mass-movement scarp, and the black dashed lines represent the extent of the deposited lobe. MS: morainic sill, DL: depositional lobe, HT: hummocky topography, and GU: gullies. Note the small-scale sediment waves on the two northern lateral banks. The acoustic sub-bottom profiles also show the horizon in which the failure occurred, the headscarp of the mass movement and its associated chaotic deposit.
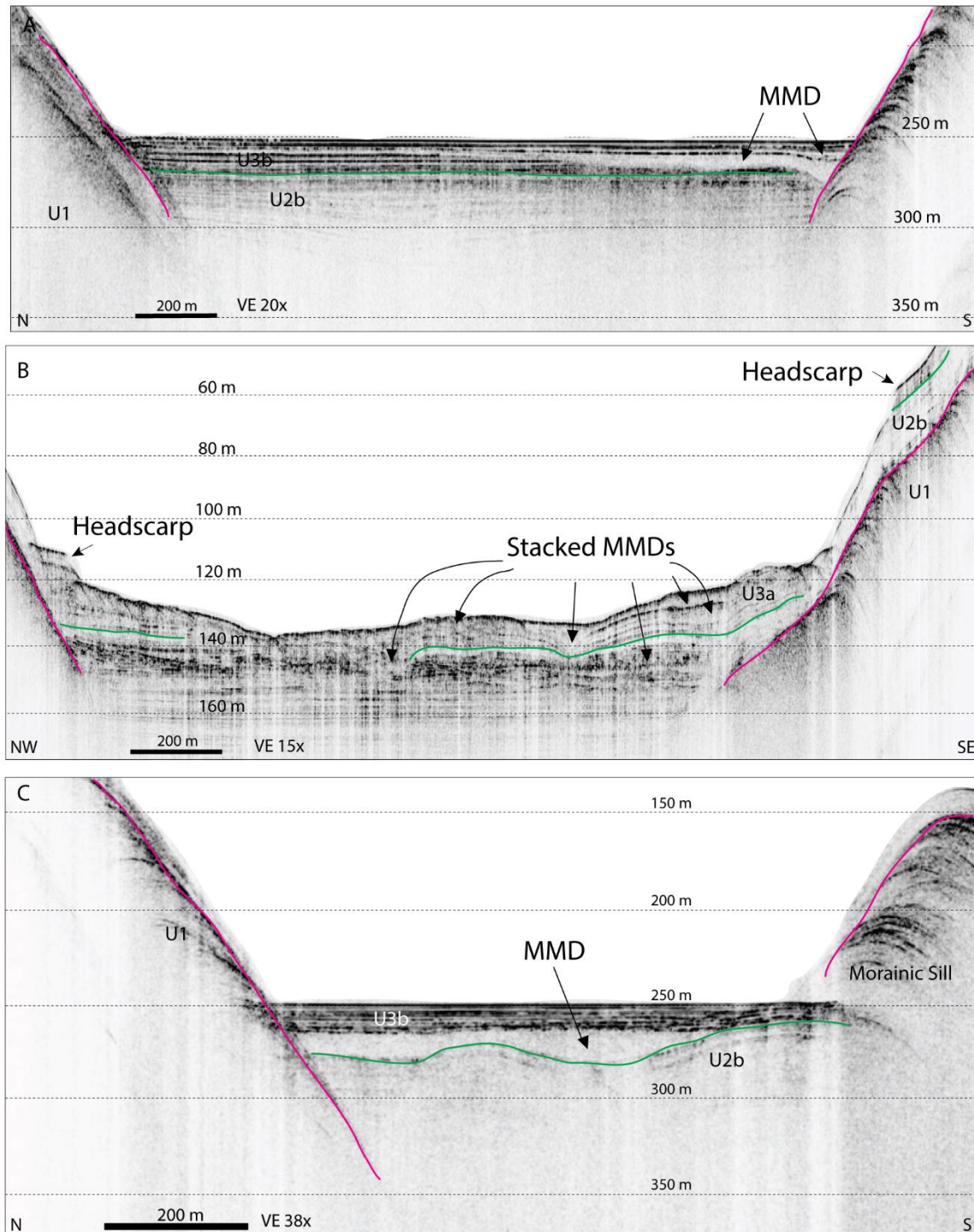
Figure 9: Three different types of MMDs in Grand Lake: small lenses at the slope toe (Profile A); stacked chaotic deposits near the Beaver River delta (Profile B); and the widespread MMD along the south-eastern margin of the central basin (Profile C).
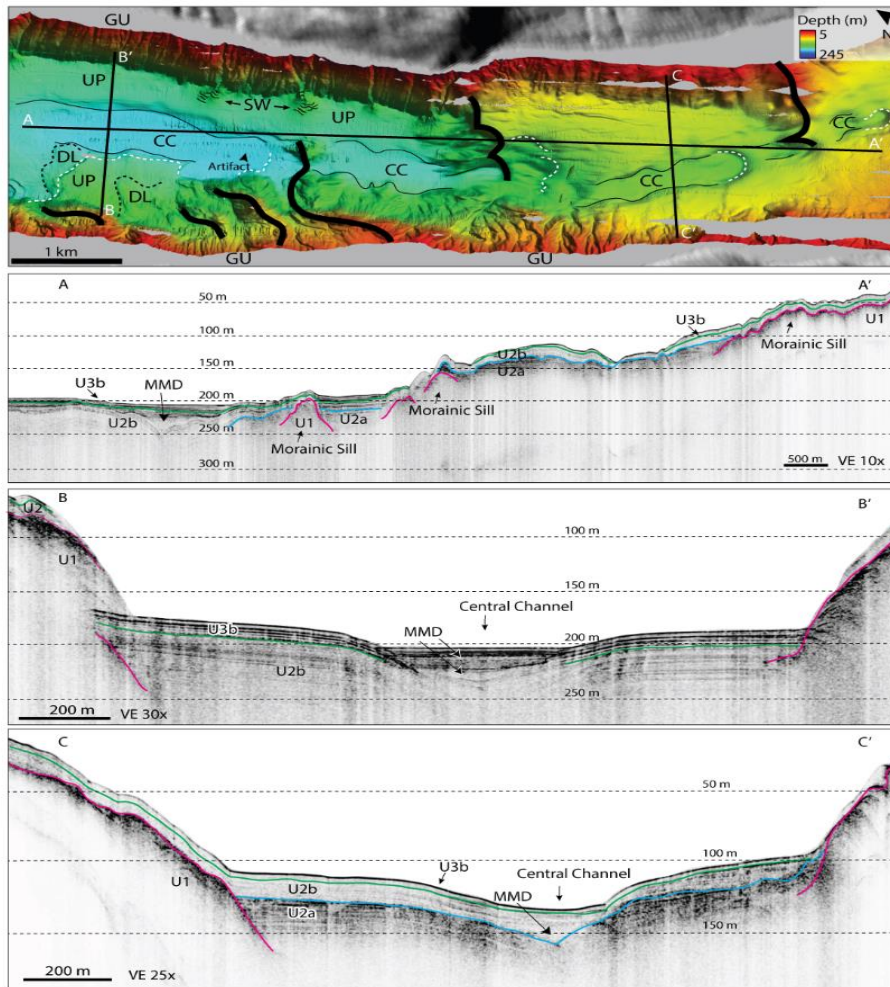
Figure 10: Swath bathymetry image and an acoustic sub-bottom profile showing the complex morphostratigraphy of the fjord-lake outlet. White dashed lines on the swath bathymetry image represent mass-movement scarps, and the extent of the deposited lobes (DL) are traced by black dashed lines. The thin black lines represent the central channel (CC) limits, and the thick black lines represent the crests of morainic sills. Other represented morphology: undisturbed plateau (UP), sediment waves (SW) and gullies (GU). Note that SW are strictly observed on small banks. The morainic sills are also shown on the acoustic sub-bottom Profile A (U1), and the central channel is shown in profiles B and C. Buried mass-movement deposits are also present in profiles B and C.
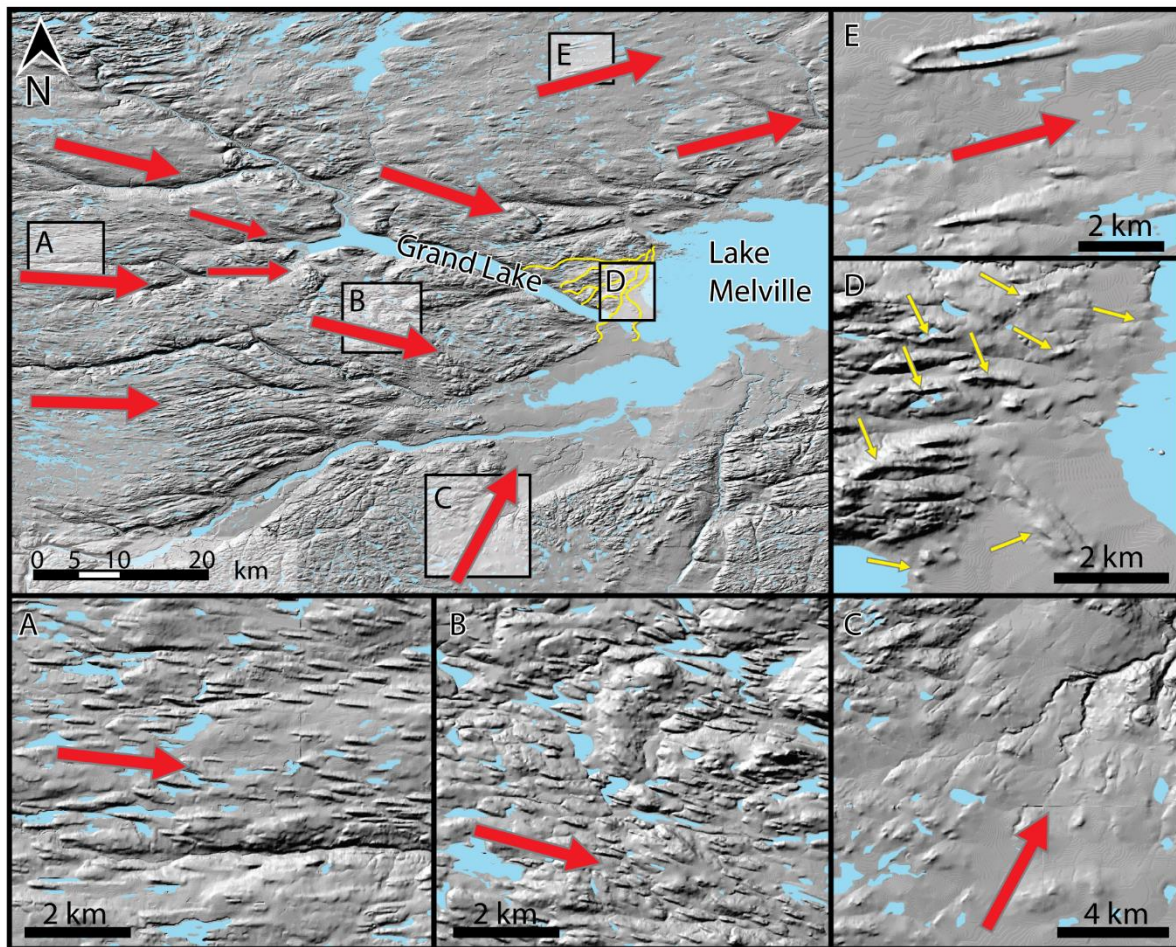
Figure 11: Glacial landforms in the area surrounding Grand Lake illustrating the direction of ice flow (red arrows). Similar small-scale glacial lineations (<1 km) are shown in A, B and C; all of these point toward Lake Melville. Note that the ice stream shown in C was reported previously by Margold et al., (2018). Larger glacial lineations (≥3 km) are shown in E, and all focus toward the NE. In C, frontal moraines are shown at the lake outlet by yellow arrows, and the moraines are traced by continuous yellow lines in the general map. The numerous glacial lineations that follow two different orientations indicate that two distinct ice streams occupied the region: one draining the Laurentide Ice Sheet toward the NE and the other draining toward Lake Melville.
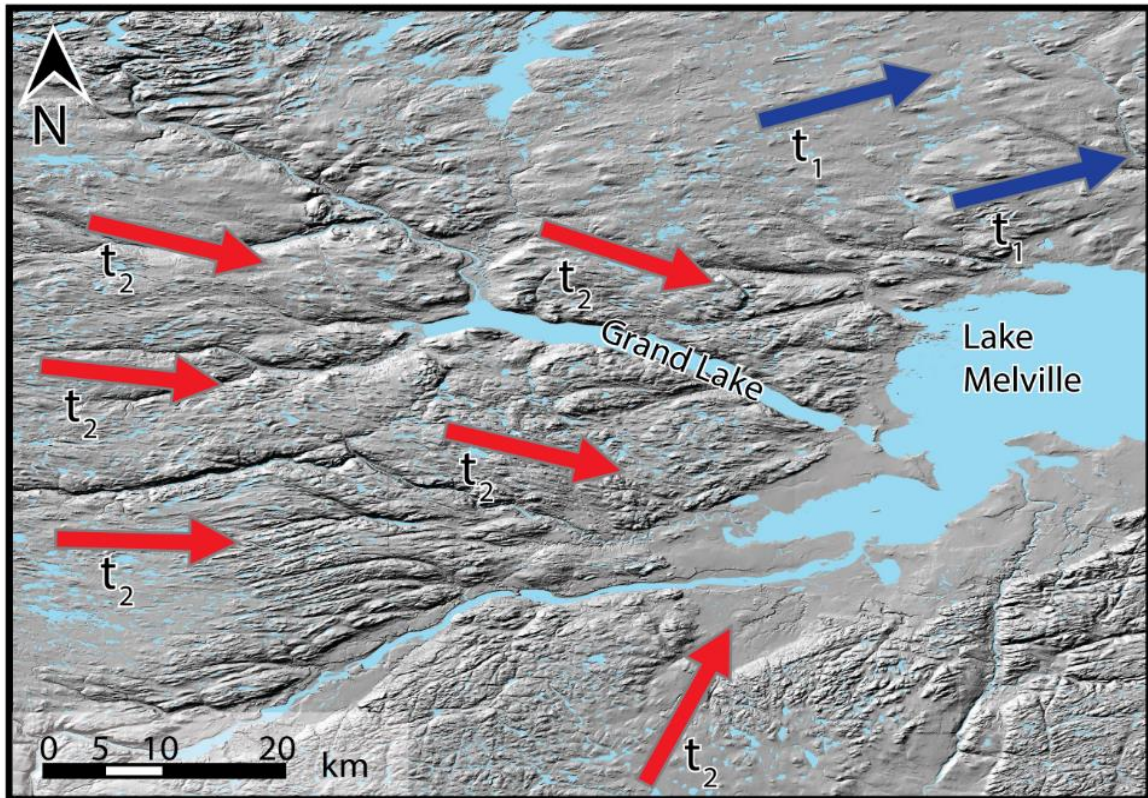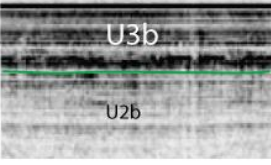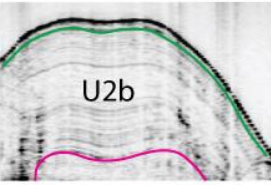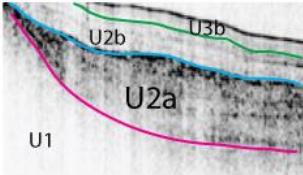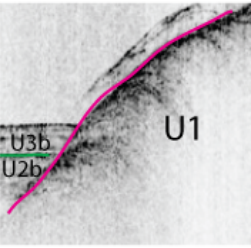
Figure 12: The timing and orientation of ice streams based on the morphology and distribution of glacial lineations. The large-scale glacial lineations observed north of Lake Melville and that point to the NE suggest that a first ice stream (t_1) drained the Laurentide Ice Sheet (LIS) toward north-eastern Labrador. The smaller scale glacial lineations focused toward Lake Melville indicate that a second (t_2) ice stream of shorter duration drained the LIS into Lake Melville. The ice drainage pattern of the LIS was reorganised during the calving bay episode of Lake Melville, shifting from ice stream t_1 to ice stream t_2.

Figure 13: Deglaciation sequence of the fjord showing the positions of ice-margin stabilisation. Note that (1) a terrestrial moraine without any sublacustrine continuity is observed between the fourth and sixth morainic sills; and (2) no ice-margin stabilisation occurred in the deep basin. The graduated arrow represents the ice retreat pattern relative to the quantity and proximity of the moraines. The first ice-margin stabilisation phase corresponds to the Sebaskachu moraine dated at ~8.2 cal ka (Fulton & Hodgson, 1979). The red star shows the location of the [10]Be dates (8.6 cal ka BP) from Ullman et al. (2016).

Table 1: Description and interpretation of acoustic units in Grand Lake, Labrador.

| Unit	Acoustic profile	Description	Interpretation
U3b		High amplitude parallel reflections closely spaced that conformably drape the underlying unit.	Distal para- and post-glacial unit
U3a		High to medium amplitude reflections interbedded by acoustically chaotic layers with an erosive base.	Deltaic sediments (para- and post-glacial unit)
U2b		Medium to low amplitude parallel reflections that conformably drape the underlying unit and is interbedded by transparent layers.	Distal glaciomarine unit
U2a		High amplitude reflections acoustically vagues.	Proximal glaciomarine unit
U1		Acoustic basement showing a high amplitude reflection.	Till/Bedrock

MORPHOLOGICAL SIGNATURES OF DEGLACIATION AND POSTGLACIAL SEDIMENTARY PROCESSES IN A DEEP FJORD-LAKE (GRAND LAKE, SOUTHEASTERN LABRADOR)

Annie-Pier Trottier*[1,2], Patrick Lajeunesse[1,2], Antoine Gagnon-Poiré[2,3] & Pierre Francus[2,3]

[1] Département de géographie, Université Laval, Québec, QC, Canada.
[2] Centre d'études nordiques (CEN), Université Laval, Québec, QC, Canada.
[3] Institut national de recherche scientifique (INRS), Centre Eau Terre et Environnement, Québec, QC, Canada
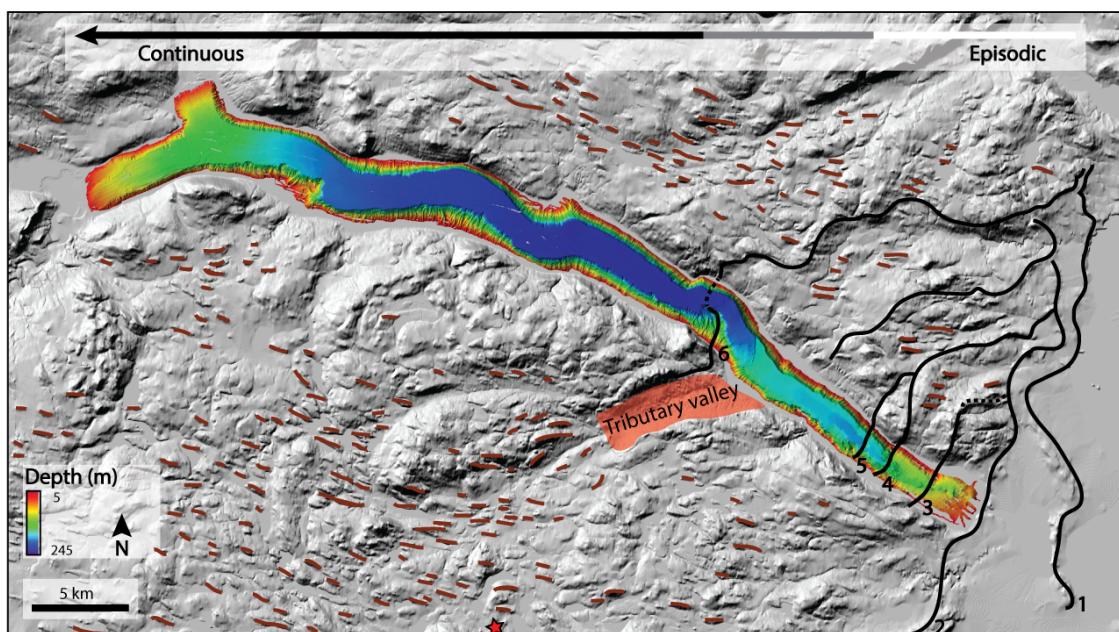
Analysis of a Digital Elevation Model (DEM), high-resolution multibeam bathymetric data and acoustic sub-bottom profiles of Grand Lake (Labrador) allowed reconstruct the retreat of the Laurentide Ice Sheet (LIS) west of Lake Melville by identifying past ice streams and a large morainic complex probably formed during the 8.2 cal ka BP cold event. The newly mapped ice streams suggest that the calving bay formed into Lake Melville triggered a reorganisation of the drainage pattern of the LIS in the area.